Dorsal raphe nucleus to anterior cingulate cortex 5-HTergic neural circuit modulates consolation and sociability

Lai-Fu Li[1,2,*], Li-Zi Zhang[1,*], Zhi-Xiong He[1], Yu-Ting Zhang[1], Huan Ma[1], Yu-Feng Xun[1], Wei Yuan[1,3], Wen-Juan Hou[1], Yi-Tong Li[1], Zi-Jian Lv[1], Rui Jia[1], Fa-Dao Tai[1,#]

[1]*Institute of Brain and Behavioral Sciences, College of Life Sciences, Shaanxi Normal University, Xi'an, 710062, China*

[2]*College of Life Sciences, Nanyang Normal University, Nanyang, 473061, China*

[3]*Provincial Key Laboratory of Acupuncture and Medications, Shaanxi University of Chinese Medicine, Xianyang 712046, China*

Running title: DR-ACC 5-HTergic neural circuit modulate consolation

*The first two authors contributed equally to this article.

#Corresponding authors: Fa-Dao Tai, PhD, Professor, College of Life Sciences, Shaanxi Normal University, Xi'an, 710062, China. E-mail: taifadao@snnu.edu.cn

ABSTRACT

Consolation is a common response to the distress of others in humans and some social animals, but the neural mechanisms underlying this behavior are not well characterized. By using socially monogamous mandarin voles, we found that optogenetic or chemogenetic inhibition of 5-HTergic neurons in the dorsal raphe nucleus (DR) or optogenetic inhibition of 5-HT terminals in the anterior cingulate cortex (ACC) significantly decreased allogrooming time in the consolation test and reduced sociability in the three-chamber test. The release of 5-HT within the ACC and the activity of DR neurons were significantly increased during allogrooming, sniffing and social approaching. Finally, we found that the activation of 5-HT1A receptors in the ACC was sufficient to reverse consolation and sociability deficits induced by the chemogenetic inhibition of 5-HTergic neurons in the DR. Our study provided first direct evidence that DR-ACC 5-HTergic neural circuit is implicated in consolation-like behaviors and sociability.

Keywords: Consolation; Empathy; Anterior cingulate cortex; Dorsal raphe nuclei; Serotonin; Fiber photometry

34 **INTRODUCTION**

35 Consolation behavior, which is referred to as an increase in affiliative contact toward a distressed
36 individual by an uninvolved bystander, is an important component of the social capabilities of
37 humans (de Waal and Preston, 2017; Field et al., 2009). Impaired consolation has been frequently
38 observed in many psychiatric diseases, such as depression, autism, and schizophrenia (Young et
39 al., 2015). According to de Waal's multilevel conceptualization of empathy (de Waal, 2008; de
40 Waal and Preston, 2017), consolation represent an intermediate level of empathy (the primary
41 level of "emotional contagion", the more complex level of "consolation", and the most elaborate
42 level of "perspective taking and targeted helping"), which has long been assumed to exist in
43 species possessing complex cognitive functions, such as humans, apes, dolphins and elephants
44 (Perez-Manrique and Gomila, 2018); however, recent studies have indicated that it also exists in
45 some socially lived rodents, such as prairie voles (Burkett et al., 2016), mandarin voles (Li et al.,
46 2019) and rats (Knapska et al., 2010).

47 Currently, studies of the neural mechanisms underlying consolation and other forms of
48 empathy have primarily focused on the oxytocin systems (Burkett et al., 2016; Li et al., 2019).
49 However, as a complex social behavior, consolation may require the coordinated actions of
50 numerous neuromodulators and neurotransmitters. Serotonin (5-HT) is an evolutionarily ancient
51 neurotransmitter that has long been implicated in a variety of emotional disorders (Faye et al.,
52 2020; Garcia-Garcia et al., 2018; Meneses and Liy-Salmeron, 2012). According to recent studies,
53 5-HT transmission is also involved in a series of social behaviors such as social interaction
54 (Walsh et al., 2018), social reward and aggression (Dolen et al., 2013). Regarding empathy, a
55 recent study revealed an association between salivary 5-HT levels and the empathic abilities of
56 people (Matsunaga et al., 2017); a polymorphism in the promoter region of the serotonin
57 transporter gene has been linked to individual differences in empathy (Gyurak et al., 2013); and
58 MDMA (±3,4-methylenedioxymethamphetamine, better known as the recreational drug
59 ''ecstasy''), which is well known to stimulate a feeling of closeness and empathy in its users
60 (Carlyle et al., 2019), had been confirmed to robustly increase the release of 5-HT in an

activity-independent manner (Heifets and Malenka, 2016). In animal studies, Kim, et al. found that microinjection of 5-HT into the anterior cingulate cortex (ACC) impairs vicarious fear and alters the regularity of neural oscillations in mice (Kim et al., 2014). Our recent study indicated that 5-HT1A receptors within the ACC are involved in consolation deficits induced by chronic social defeat stress in mandarin voles (Li et al., 2020). However, to our knowledge, direct evidence for an association between 5-HT and consolation has yet to be obtained.

Dorsal raphe nucleus (DR) is a main source of 5-HT neurons and provide 70% of 5-HTergic projections in the forebrain (Fu et al., 2010; Luo et al., 2015). DR 5-HTergic neurons form dense, broad and bidirectional neural connections with a broad range of forebrain and limbic structures, including the ACC (Celada et al., 2013; Charnay and Leger, 2010), which is a central hub for various types of empathy. Therefore, direct modulation of the DR→ACC 5-HTergic circuit to investigate its function role in consolation-like behaviors is interesting and meaningful.

The released 5-HT binds to pre- and postsynaptic receptors. To date, at least 14 different 5-HT receptor subtypes have been identified in the brain (Artigas, 2013). Among which, 5HT1AR and 5HT2AR are the two main subtypes that are expressed at high levels in the prefrontal cortex (Carhart-Harris and Nutt, 2017; Santana and Artigas, 2017). The distribution, signaling pathways and functions of these two receptors are substantially different, and both receptors play critical roles in modulating cortical activity and neural oscillations (Celada et al., 2013). Previous studies indicated that 5HT2AR gene single nucleotide polymorphisms are associated with empathy-related social communication abilities (Gong et al., 2015), and a 5HT2AR agonist increases emotional empathic ability (Dolder et al., 2017). However, in animal studies by Kim, et al., blockade of serotonin receptors in the ACC did not affect observational fear responses in mice (Kim et al., 2014). Clearly, the specific functions of 5HT1AR and 5HT2AR in empathy-like behaviors still require further examination.

The mandarin vole (*Microtus mandarinus*) is a socially monogamous rodent that is widely distributed across China (He et al., 2019). As shown in our previous studies, this species is capable of displaying consolation-like behaviors upon exposure to a distressed partner (Li et al.,

88 2020; Li et al., 2019). In the present study, we first investigated the function of DR→ACC
89 5-HTergic circuits in consolation-like behavior using optogenetic and chemogenetic approaches.
90 To provide more direct evidence, we then monitored ACC 5-HT release and DR neuron activities
91 during this behavior by using *in vivo* fiber photometry. Finally, we used chemogenetics plus
92 pharmacological approaches to investigate which types of 5-HT receptors in the ACC are
93 involved in consolation-like behaviors in mandarin voles. In order to investigate any potential
94 sex differences during these processes, both male and female subjects were included in our study.
95 As consolation is in general a pro-social behavior, some social behaviors were investigated
96 during the tests.

97 **RESULTS**

98 **Optogenetic inhibition of DR 5-HT neurons in the DR→ACC neural circuit impaired**
99 **consolation and reduced sociability**

100 We first determined the 5-HTergic projection relationship between the DR and ACC in mandarin
101 voles. For this experiment, the retrograde tracer CTB was injected into the ACC, followed by
102 immunofluorescence staining of the DR sections with TPH2, a marker of 5-HTergic neurons. A
103 substantial number of TPH2+ neurons colocalized with CTB, indicating the presence of DR-ACC
104 5-HTergic projections (Figure 1—figure supplement 1). We then used a novel dual-virus
105 optogenetics approach to explore the function of the DR-ACC 5-HTergic circuit in
106 consolation-like behaviors and sociability, where double-floxed AAV-DIO-ChR2-mCherry
107 (DIO-ChR2) or AAV-DIO-eNpHR3.0-mCherry (DIO-eNpHR3.0) was injected into the DR and
108 retro-AAVs containing the TPH2 promoter and Cre element (rAAV(Retro)-TPH2-Cre) were
109 injected into the ACC (Figure 1A). This virus strategy ensures that opsins (excitatory CHR2 or
110 inhibitory eNpHR3.0) are mainly expressed within the DR-ACC 5-HTergic circuit.
111 Immunohistochemical staining showed that more than 75% of mCherry-labeled neurons
112 expressed TPH2 in both male and female voles, and more than 80% of TPH2+ cells coexpressed
113 mCherry (Figure 1—figure supplement 2). In the electrophysiological study, we found that the

114 DR neurons reliably responded to pulses of 473 (activation)/593 (inhibition) nm light stimuli
115 (Figure 1D-E). These results indicate the viability of this virus strategy.
116 To test whether modulation of DR 5-HT neuron activity alters consolation and sociability,
117 five weeks after the virus injection, optic fibers were implanted above the DR (Figure 1A-B). The
118 virus expression sites and the optic fiber placement schematics are shown in Figure 1—figure
119 supplement 3A. According to Burkett's and our previous results (Burkett et al., 2016; Li et al.,
120 2019), the time spent grooming their stressed partners (allogrooming) is an important indicator
121 of consolation-like behaviors. We then exposed the subjects to their electric-shocked partners and
122 recorded the time spent allogrooming, chasing (closely following) and selfgrooming (consolation
123 test; for details, please refer to the Methods section). The three-chamber test was used to assay
124 the sociability along with open-field anxiety and locomotion (Figure 1B). In the CHR2-expressing
125 animals, there was no conclusive evidence that optogenetic activation of 5-HTergic neurons
126 affected their time spent allogrooming, chasing and self-grooming in the 10-min consolation test
127 (Figure 1G, Figure 1—figure supplement 4A-D), the social interaction ratio in the 3-chamber test
128 (Figure 1I), and behavioral performance in the open-field test (Figure 1K, Figure 1—figure
129 supplement 4E).
130 However, in the eNPHR3.0-expressing animals, there was extremely strong evidence that
131 optogenetic inhibition of 5-HT neurons in the DR reduced the time spent allogrooming (Figure
132 1H) and chasing (Figure 1—figure supplement 4B), but had little effect on the control behavior
133 self-grooming (Figure 1—figure supplement 4D). Following experiments indicated that the
134 light-inhibition effects significantly reduced within 24 h (Figure 1—figure supplement 5). In the
135 3-chamber test, light inhibition also significantly reduced the social preference ratio (Figure 1J).
136 In the open-field test, the results were inconclusive, which suggests that the data for the time
137 spent in the central area and the total distance travelled are equally likely under H0 and H1
138 (Figure 1L, Figure 1—figure supplement 4F).
139 The above results indicate that although we have no conclusive results for optogenetic
140 activation, optogenetic inhibition of 5-HT neurons within the DR→ACC 5-HTergic circuit

impaired consolation-like behavior and sociability in mandarin voles.

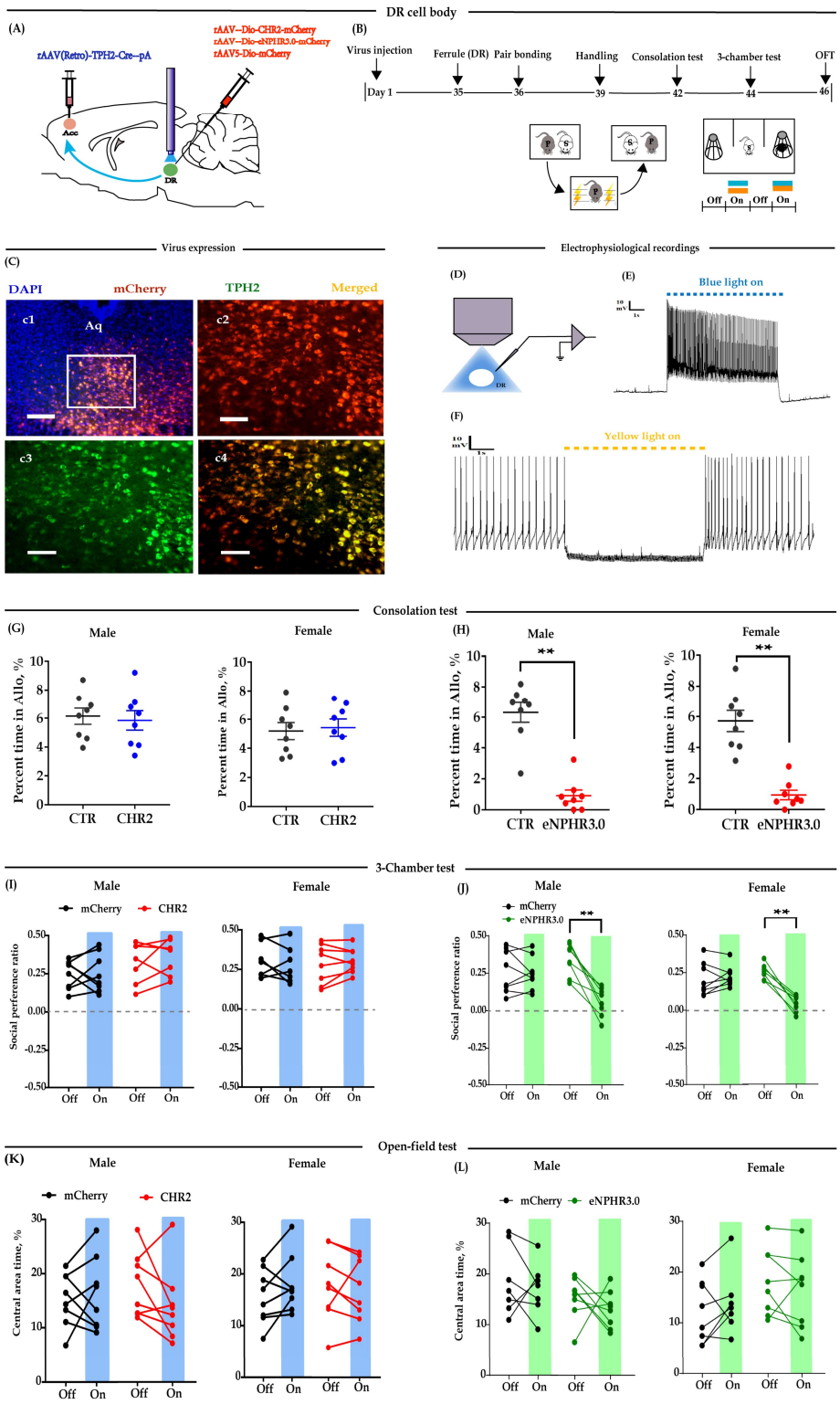

Figure 1. Optogenetic bidirectional modulation of 5-HT neuron in the DR in the DR-ACC

neural circuit. (A): Schematic of optogenetic manipulation; (B): timeline of experiments; (C): immunohistological image showing virus expression in the DR (c1, × 100) and amplified images in the left box showing the mCherry, TPH2 and the colocaliztion of the two ('c2-c4', × 200); (D): electrophysiological recordings model; (E & F): representative traces from electrophysiological recordings showing photostimulation (E) and photoinhibition of a 5-HT neuron (F); (G-L): quantification of allogrooming time in the consolation test (G & H); social preference ratio in the three-chamber test (I & J) and time spent in the central area in the open-field test (K & L) during optogenetic modulations. Data are presented as mean ± SE, n = 7–8 in each group, $^{**}P < 0.01$. For 'G-H', independent samples t tests along with Bayesian independent samples t-test; for 'I-L', two-way repeated measures ANOVA along with two-way repeated Bayesian measures ANOVA (light as within subject factor). For raw data in this figure, please refer to Figure 1—source data 1. For detailed quantifications, please refer to Supplementary 2. ACC: anterior cingulate cortex; CTR: control; DR: dorsal raphe nucleus; TPH2: tryptophan hydroxylase 2.

161 **Optogenetic inhibition of ACC 5-HT terminals in the DR→ACC neural circuit similarly**
162 **impaired consolation and reduced sociability**
163 Modulation of 5-HT neurons may affect other neurons in the DR, and thus confound behavioral
164 performance. In subsequent experiments, we placed optic fibers in the ACC and investigated
165 whether the direct modulation of 5-HT terminals in this region would exert the same effects
166 (Figure 2A). Similarly, we found that optogenetic activation of DR-ACC 5-HT terminals did not
167 significantly alter behavioral performance in the consolation test (Figure 2C, Figure 2—figure
168 supplement 1A, 1C) and open-field test (Figure 2G, Figure 2—figure supplement 1E). In the
169 3-chamber test, two-way repeated measures ANOVA revealed a moderate 'light × group'
170 interaction in females ($F_{(1,14)} = 6.297$, $P = 0.025$, $BF_{incl} = 4.186$). Subsequent *post hoc* comparison
171 results showed that light stimulation slightly increased the social preference ratio in
172 CHR2-expressing females but not in mCherry-expressing females (ChR2: off *vs*. on, $P = 0.033$;
173 mCherry: off *vs*. on, $P = 0.975$; Figure 2E). The 'light × group' interaction was not evidently
174 observed in males ($F_{(1,14)} = 3.556$, $P = 0.08$, $BF_{incl} = 1.239$).
175 Optogenetic inhibition of DR-ACC 5-HT terminals significantly reduced the time spent
176 allogrooming and chasing in the consolation test (Figure 2D, Figure 2—figure supplement 1B)
177 and the social preference ratio in the 3-chamber test (Figure 2F). Similarly, the inhibition had
178 little effect on the control behavior of selfgrooming (Figure 2—figure supplement 1D) and
179 behavioral performance in open-field test (Figure 2H, Figure 2—figure supplement 1F) and the
180 inhibitory effect lasted no more than 24 h (Figure 2—figure supplement 2). The above results
181 indicated that optogenetic modulation of ACC 5-HT terminals have nearly identical effects as
182 modulation of DR 5-HT neurons.
183
184
185
186
187

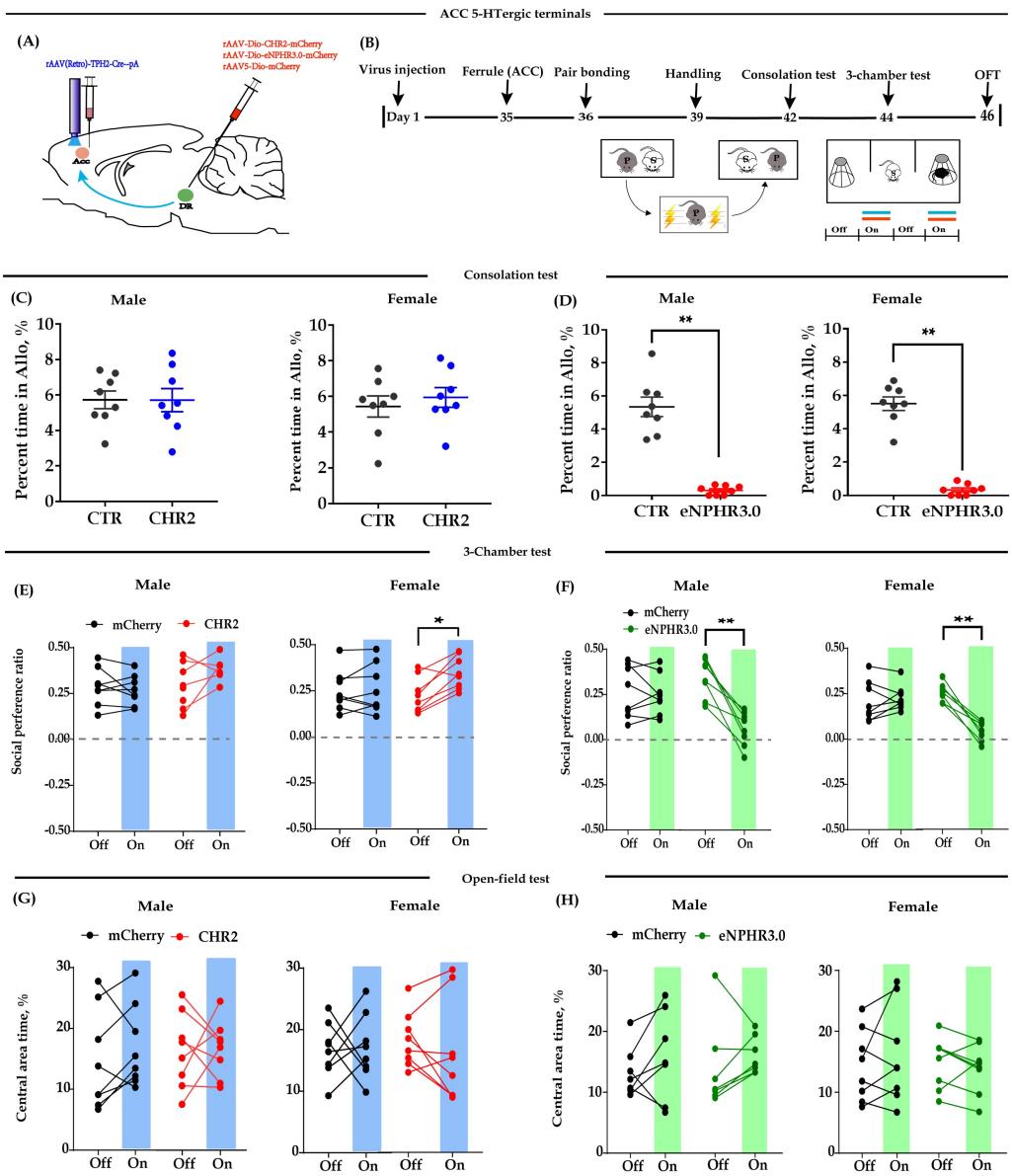

188

189 **Figure 2. Optogenetic bidirectional modulation of 5-HT terminals within the ACC in the**

190 **DR-ACC neural circuit.** (A): Schematic of optogenetic manipulation; (B): timeline of experiments;

191 (C-H): quantification of time spent in allogrooming in the consolation test (C & D), sociability in

192 the three-chamber test (E & F) and time spent in the central area in the open-field test (G & H)

193 during optogenetic modulations. Data are presented as mean ± SE, n = 7–8 in each group, *P <

194 0.05, **P < 0.01. For C-D, independent samples t tests along with Bayesian independent samples

195 t-test; for E-H, two-way repeated measures ANOVA along with two-way repeated Bayesian

196 measures ANOVA (light as within subject factor). For raw data in this figure, please refer to

197 Figure 2—source data 1. For detailed quantifications, please refer to Supplementary 2. ACC:

198 anterior cingulate cortex; DR: dorsal raphe nucleus; CTR: control.

199

200 **Chemogenetic inhibition of DR 5-HT neurons in the DR→ACC neural circuit impaired**
201 **consolation and reduced sociability**

202 To confirm the above optogenetic results over a longer time frame, we used a chemogenetic
203 approach to selectively express 'Gq-DREADD' or 'Gi-DREADD' in DR 5-HT neurons by injecting
204 AAV-DIO-hM4Dq-mCherry (Gq-DREADD) or AAV-DIO-hM4Di-mCherry (Gi-DREADD) into
205 the DR and rAAV(Retro)-TPH2-Cre into the ACC (Figure 3A). Immunohistochemical staining
206 revealed that more than 65% of TPH2 labeled neurons were infected by mCherry virus and more
207 than 60% of mCherry cells coexpressed TPH2 (Figure 3—figure supplement 1). The virus
208 expression sites schematics were shown in Figure 1—figure supplement 3B. To determine
209 whether the ligand CNO can activate or inhibit DR 5-HT neurons, whole-cell current-clamp
210 recordings were performed. The results showed that the addition of 10 μM CNO remarkably
211 increased the number of action potentials in the Gq-DREADD-transfected neurons (Figure 3D).
212 In contrast, CNO caused a significantly decrease in the number of spikes (Figure 3E) and
213 increased the spike rheobase during current step injections in Gi-DREADD-transfected neurons
214 (Figure 3F). These results indicate the specificity and viability of this virus strategy.

215 In subsequent behavioral studies, we found CNO (1 mg/kg, i.p.) treated
216 Gi-DREADD-expressing voles showed reduced grooming toward their shocked partners in the
217 consolation test (Figure 3G) and decreased sociability in the 3-chamber test (Figure 3H). The
218 CNO treated males also showed a trend of spending less time in the open-field test, but the
219 statistics were inconclusive (Figure 3I; treatment: $F_{(1,19)} = 4.305$, $P = 0.052$, BF(incl) = 4.438; Group:
220 $F_{(2,19)} = 2.064$, $P = 0.155$, BF(incl) = 0.384; treatment × Group: $F_{(1,19)} = 0.164$, $P = 0.850$, BF(incl) =
221 0.300). The treatment had no detectable effects on the total distance travelled in the open-field
222 test (Figure 3—figure supplement 2C) and some control behaviors in the consolation test (Figure
223 3—figure supplement 2A&B). In Gq-DREADD and virus control subjects, CNO treatment had no
224 detectable effects on the behavioral performance in all the test (Figure 3).

225 Based on the results of the chemogenetic and optogenetic experiments described above, we

226 concluded that inhibition of DR-ACC 5-HTergic circuit activity was sufficient to impair

227 consolation and sociability in mandarin voles.

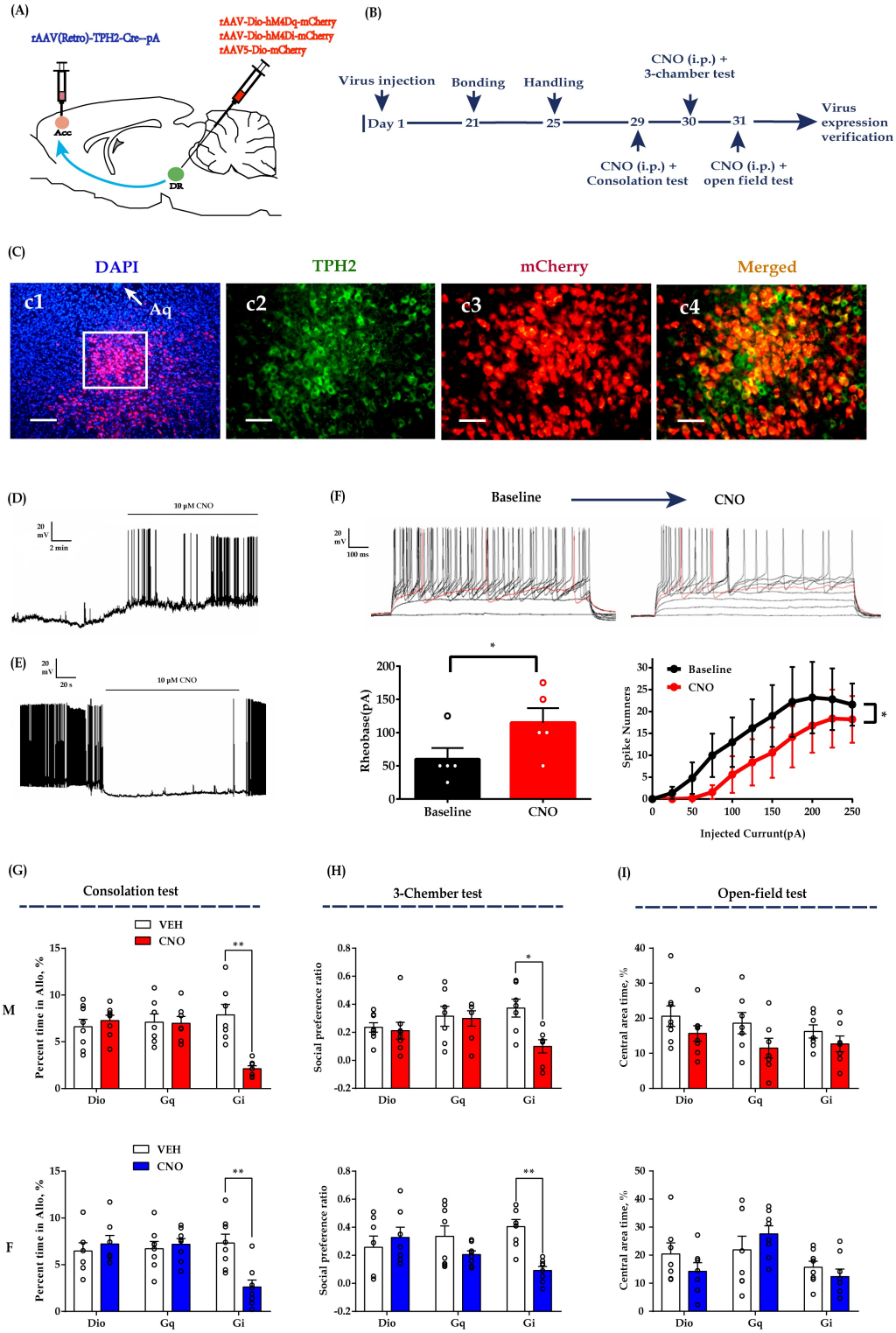

228

229 **Figure 3. Chemogenetic modulation of DR 5-HT neuron activities in the DR-ACC neural**
230 **circuit.** (A): Schematic of chemogenetical manipulations; (B): timeline of experiments; (C):
231 immunohistological image showing virus expression in the DR (c1, × 100) and amplified images
232 in the left white box showing the mCherry, TPH2 and the colocaliztion of the two (c2-c4, × 200);
233 (D): representative trace from a Gq-DREADD neuron; (E): representative trace from a
234 Gi-DREADD-transfected neuron; (F): quantification of spike rheobase and spike numbers under
235 current step injections in Gi-DREADD-transfected neurons (n = 5 neurons, *P < 0.05); (G-I):
236 quantification of allogrooming time in the consolation test (G); social preference ratio in the
237 three-chamber test (H) and time spent in the central area in the open-field test (I) in male (upper
238 panels) and female (down panels) voles. Data are presented as mean ± SE, n = 7–8 in each group,
239 *P < 0.05, **P < 0.01 compared with vehicle control. For 'F', one tailed paired t test along with one
240 tailed Bayesian paired samples t-test; for 'G-I', two-way repeated measures ANOVA along with
241 two-way repeated Bayesian measures ANOVA. For raw data in this figure, please refer to Figure
242 3—source data 1. For detailed quantifications, please refer to Supplementary 2. ACC: anterior
243 cingulate cortex; DR: dorsal raphe nucleus; TPH2: tryptophan hydroxylase 2; M: male; F: female.

244 **DR 5-HT neuron activity increased during allogrooming and social approaching**
245 If the DR-ACC 5-HTergic circuit is involved in consolation and sociability, ACC projecting DR
246 5-HT neurons may change their activity during the corresponding behaviors. To verify this idea,
247 we performed photometric recording in freely moving animals by injecting Cre-inducible
248 AAV-DIO-GCaMp6, a genetically encoded fluorescent Ca^{2+} sensor, into the DR and
249 rAAV(Retro)-TPH2-Cre into the ACC (Figure 4A). Ten days later, fibers were implanted above
250 the DR injection sites. Post hoc histological analysis revealed that more than 80% $GCaMp6^{+}$ cells
251 overlapped with $TPH2^{+}$ expressing cells (Figure 4—figure supplement 1). The virus expression
252 sites and the optic fiber placements schematics were shown in Figure 1—figure supplement 3C.
253 During the consolation test, we found that the activity of DR 5-HT neurons was reliably
254 increased during allogrooming, social approaching and sniffing in both sexes (Figure 4E1-E2,

255 F1-F2 and G1-G2). DR 5-HT neurons showed the highest response during allogrooming which
256 may indicate the specific role of 5-HT in consolation-like behaviors (Figure 4—figure supplement
257 2A-2B). Interesting, the increased Ca^{2+} in DR 5-HT neurons often preceded these behaviors
258 which may indicate the motivational function of 5HT (Arakawa, 2020; Yagishita, 2020). When
259 aligning the fluorescence changes to the end of these social bouts, we found that the activity of
260 5-HT neurons decreased accordingly before withdrawal from allogrooming and approaching
261 (Figure 4—figure supplement 3A-3B). Withdrawing from sniffing also showed a similar trend
262 but was not statistically significant (Figure 4—figure supplement 3C; pre *vs*. post: male: $t_{(5)} = 1.611$,
263 $P = 0.084$, BF+0 = 1.589 with median posterior $\delta = 0.528$, 95%CI = [0.041, 1.363]; female: $t_{(5)} = 1.724$, P
264 $= 0.073$, BF+0 = 1.778 with median posterior $\delta = 0.557$, 95%CI = [0.046, 1.415]). The increased activity
265 of DR 5-HT neurons did not simply reflect movement initiation as no fluorescence changes were
266 observed when aligning to running and selfgrooming (Figure 4H1-H2, I1-I2). Furthermore, no
267 significant changes in fluorescence signals were detected in DR 5-HT neurons of GFP-expressing
268 control voles during all the behaviors, confirming that the GCaMp6 signals genuinely indicated
269 neuronal activity and did not simply reflecting motion artifacts (Figure 4E3-E4, F3-F4, G3-G4,
270 H3-H4 and I3-I4).
271 The above results provide direct evidence that DR 5-HT neurons within the DR-ACC
272 5-HTergic circuit are recruited in consolation-like behavior and sociability in mandarin voles.
273
274
275

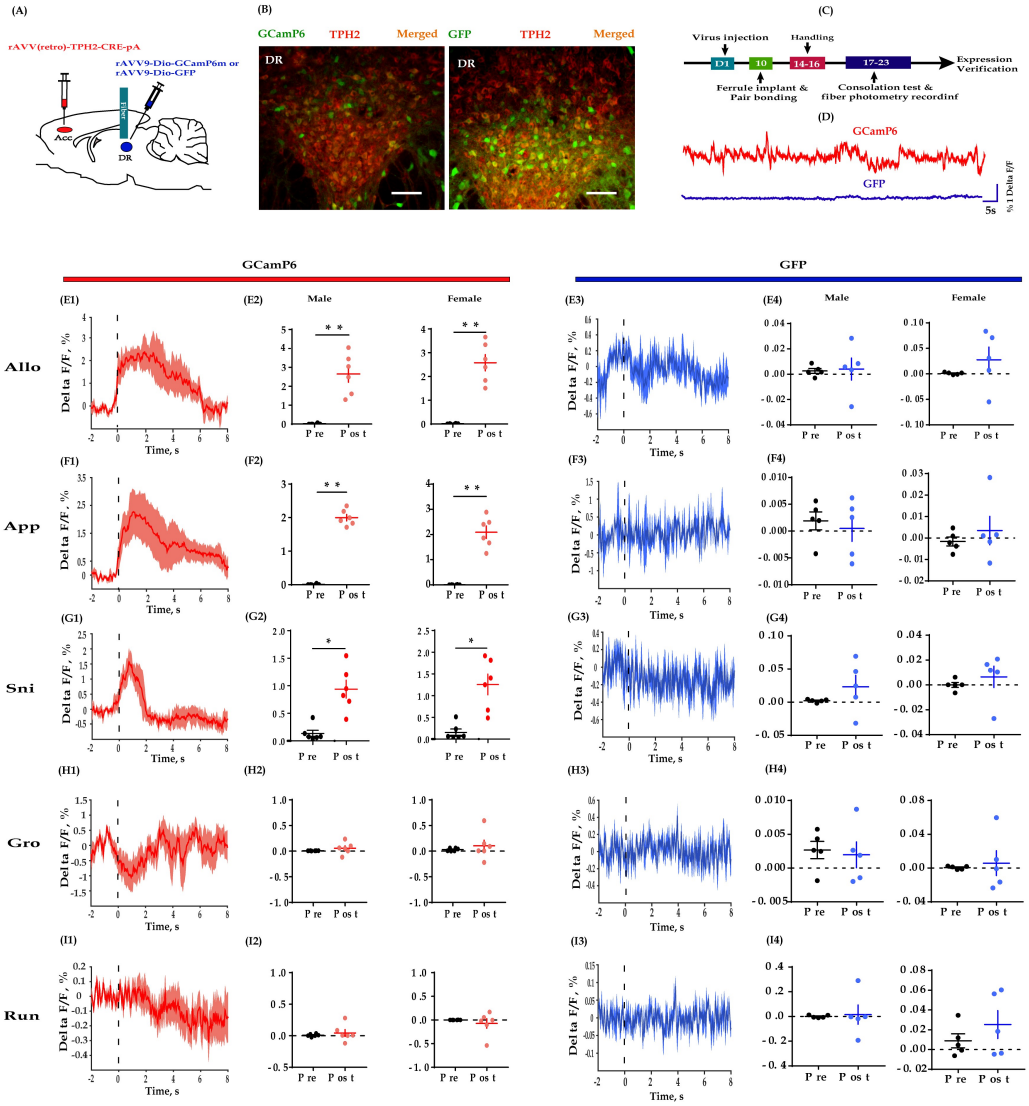

Figure 4. Fiber photometry recording DR 5-HT neural dynamics during the consolation test. (A): Schematic diagrams depicting the virus injection and recording sites; (B): histology showing the expression of GCaMP6 (left) and GFP control (right) in the DR (× 200); (C): experimental timeline for photometry experiments; (D): representative fluorescence changes of GCaMP6 (red line) and GFP (blue line) during photometry recordings; (E1-I1): representative peri-event plot of GCaMP6 fluorescence signals aligned to onsets of various behavior (for all peri-event plots, the red line denotes the mean signals of 4-6 bouts of behaviors, whereas the red shaded region denotes the SE); (E2-I2): quantification of change in GCaMP6 fluorescence signals before and after the events (*n* =6 in each group); (E3-I3): representative peri-event plot of GFP signals aligned to onsets of various behavioral events (for all peri-event plots, the blue line denotes the

287 mean signals of 4-6 bouts of behaviors, whereas the blue shaded region denotes the SE); (E4-I4):
288 quantification of change in GFP fluorescence signals before and after the events (n = 5 in each
289 group). Data are presented as mean ± SE, *P < 0.05, **P < 0.01, Paired samples t-test along with
290 Bayesian paired samples t-test. For raw data in this figure, please refer to Figure 4—source data 1.
291 For detailed quantifications, please refer to Supplementary 2. ACC: anterior cingulate cortex;
292 TPH2: tryptophan hydroxylase 2; Allo: allogrooming; Sni: sniffing; App: approaching; Gro:
293 selfgrooming; Run: running.

294 **ACC 5-HT release increased during allogrooming, social approach and sniffing**

295 To further establish the potential relevance of 5-HT in consolation-like behaviors, we directly
296 detected the dynamics of 5-HT within the ACC using a newly developed GPCR-activation-based
297 5-HT sensor along with photometric recording (Wan, *et al* 2020). To do this, we injected AAV
298 encoding the fluorescent 5-HT sensor (AAV-5HTsensor 2.1) unilaterally into the ACC and
299 implanted optic fibers above the injection site ten days later (Figure 5A). The virus expression
300 sites and the optic fiber placements schematics were shown in Figure 1—figure supplement 3D.
301 Control animals were injected with AAVs encoding eGFP. Post hoc histological verification
302 indicated expression of both the 5-HT sensor and eGFP within the ACC (Figure 5B).

303 Next, we measured the dynamics of endogenous 5-HT during the consolation test.
304 Consistent with the above fiber photometry of Ca^{2+} signals in DR 5-HT neurons, we found
305 reliably increased fluctuations in fluorescence within the ACC in conjunction with allogrooming,
306 social approaching and sniffing, but not observed with self-grooming and running (Figure 5, left
307 columns). Similarly, the peek 5-HT signals during allogrooming were larger than during the
308 other behaviors (Figure 4—figure supplement 2C-2D), and the release of 5-HT significantly
309 dropped before the end of allogrooming, approaching and sniffing (Figure 5—figure supplement
310 1). In control animals that expressed GFP in the ACC, we observed little fluorescence change
311 during any of these behaviors (Figure 5E3-E4, F3-F4, G3-G4, H3-H4 and I3-I4).

312 To validate the selectivity of this 5-HT sensor in mandarin voles, in another set of animals

expressing the 5-HT sensor, a 5-HT receptor antagonist metergoline (Met) was injected (i.p., 4 mg/kg) before conducting the fiber photometry experiments. We found that treating voles with Met completely blocked the fluorescence changes of the 5-HT sensor during allogrooming (Figure 5—figure supplement 2), validating the viability and specificity of this 5-HT sensors.

The above results provide further evidence that 5-HT released within the ACC may play an important role in consolation-like behavior and sociability in mandarin voles.

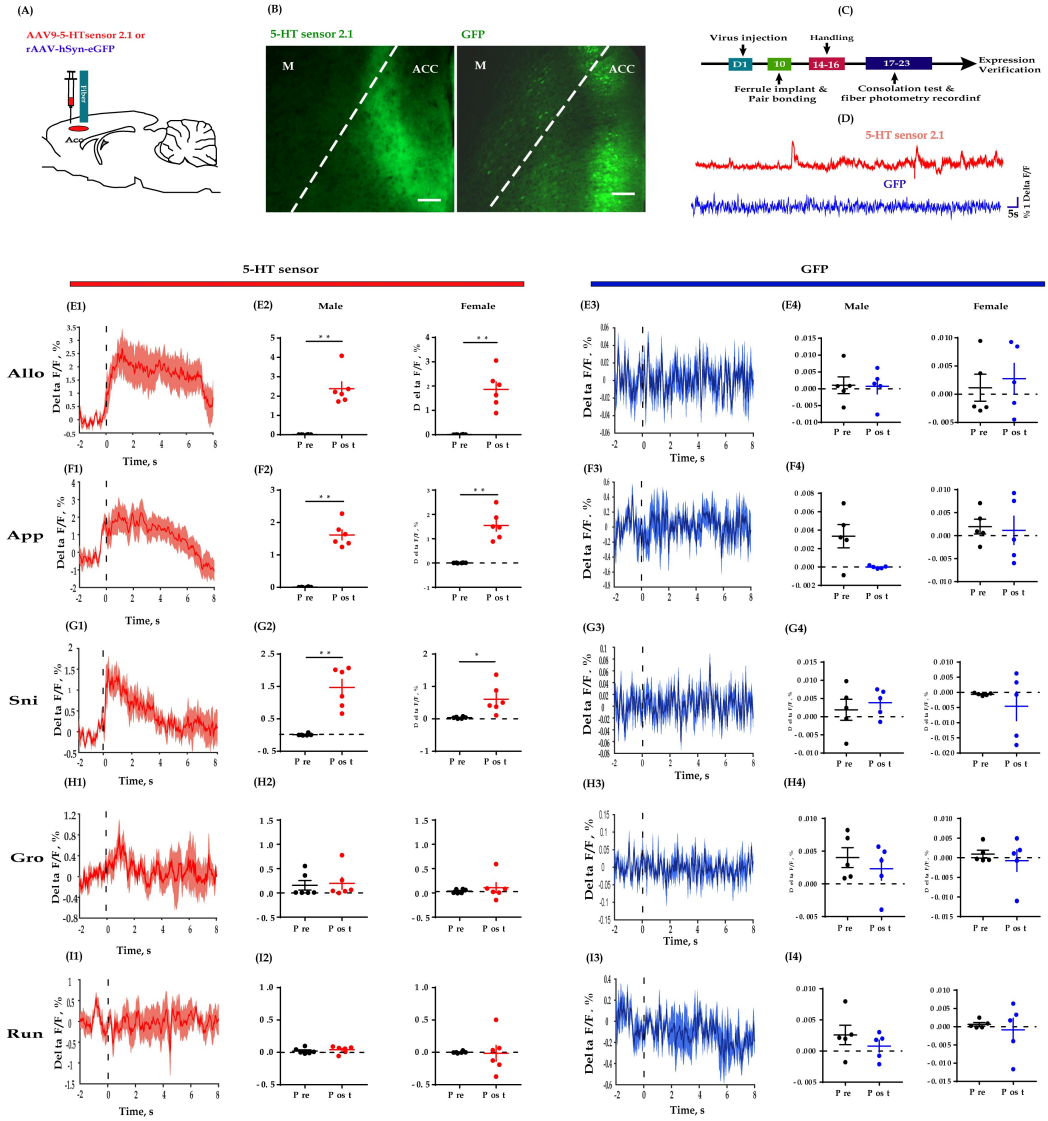

Figure 5. Fiber photometry recording dynamics of 5-HT within the ACC during the consolation test. (A): Schematic diagrams depicting the virus injection and recording sites; (B): histology showing the expression of 5-HT sensor (left) and GFP control (right) within the ACC (×

323 200); (C): experimental timeline for photometry experiments; (D): representative fluorescence
324 changes of 5-HT sensor (red line) and GFP (blue line) during photometry recordings; (E1-I1):
325 representative peri-event plot of 5-HT fluorescence signals aligned to onsets of various behavior
326 (for all peri-event plots, the red line denotes the mean signals of 4-6 bouts of behaviors, whereas
327 the red shaded region denotes the SE); (E2-I2): quantification of change in 5-HT fluorescence
328 signals before and after the events (n = 6 in each group); (E3-I3): representative peri-event plot of
329 GFP signals aligned to onsets of various behavioral events (for all peri-event plots, the blue line
330 denotes the mean signals of 4-6 bouts of behaviors, whereas the blue shaded region denotes the
331 SE); (E4-I4): quantification of change in GFP fluorescence signals before and after the events (n =
332 5 in each group). Data are presented as mean ± SE, *P < 0.05, **P < 0.01; paired samples t-test
333 along with Bayesian paired samples t-test. For raw data in this figure, please refer to Figure
334 5—source data 1. For detailed quantifications, please refer to Supplementary 2. ACC: anterior
335 cingulate cortex; M: motor cortex; TPH2: tryptophan hydroxylase 2; Allo: allogrooming; Sni:
336 sniffing; App: approaching; Gro: selfgrooming; Run: running.

337 **Serotonin in the ACC mediated consolation-like behaviors through 5-HT1A receptors**

338 The most abundant 5-HT receptors expressed in the mPFC are 5-HT1AR and 5-HT2AR
339 (Carhart-Harris and Nutt, 2017). Increasing evidence indicates that these two types of receptors
340 exert opposite effects within the mPFC (Celada et al., 2013; Puig and Gulledge, 2011). In our
341 previous study, we indicated that ACC administration of a 5HT1AR agonist (8-OH-DPAT)
342 rescued the impaired consolation and sociability induced by social defeat (Li et al., 2020). To
343 further examine which receptor mediates consolation-like behaviors within the ACC, we directly
344 infused 8-OH-DPAT (200 nL/side; 1.5 mg/mL) or a 5-HT2AR antagonist (MDL 100907, 200
345 nL/side; 1 mg/mL) into the ACC along with chemogenetic inhibition of DR 5-HT neurons
346 before conducting behavioral assays (Figure 6A & B). Not surprisingly, CNO elicited deficits in
347 allogrooming and sociability (Figure 6C, D, F, G: left two bars). Pretreatment with 8-OH-DPAT
348 significantly reduced the impact of CNO (Figure 6C, D: right two bars; see also the comparison

349 results of 'Vehicle+Saline - Vehicle+CNO' *vs.* '8-OH-DPAT+Saline - 8-OH-DPAT+CNO'; Figure

350 6—figure supplement 1A, B), whereas MDL 100907 had no such effect (Figure 5F, G: right two

351 bars; Figure 6—figure supplement 1C, D). Neither the drugs nor viruses had any detectable

352 effect on the control behavior of self-grooming or behavioral performance in the open-field test

353 (Figure 6E-H, Figure 6—figure supplement 2).

354

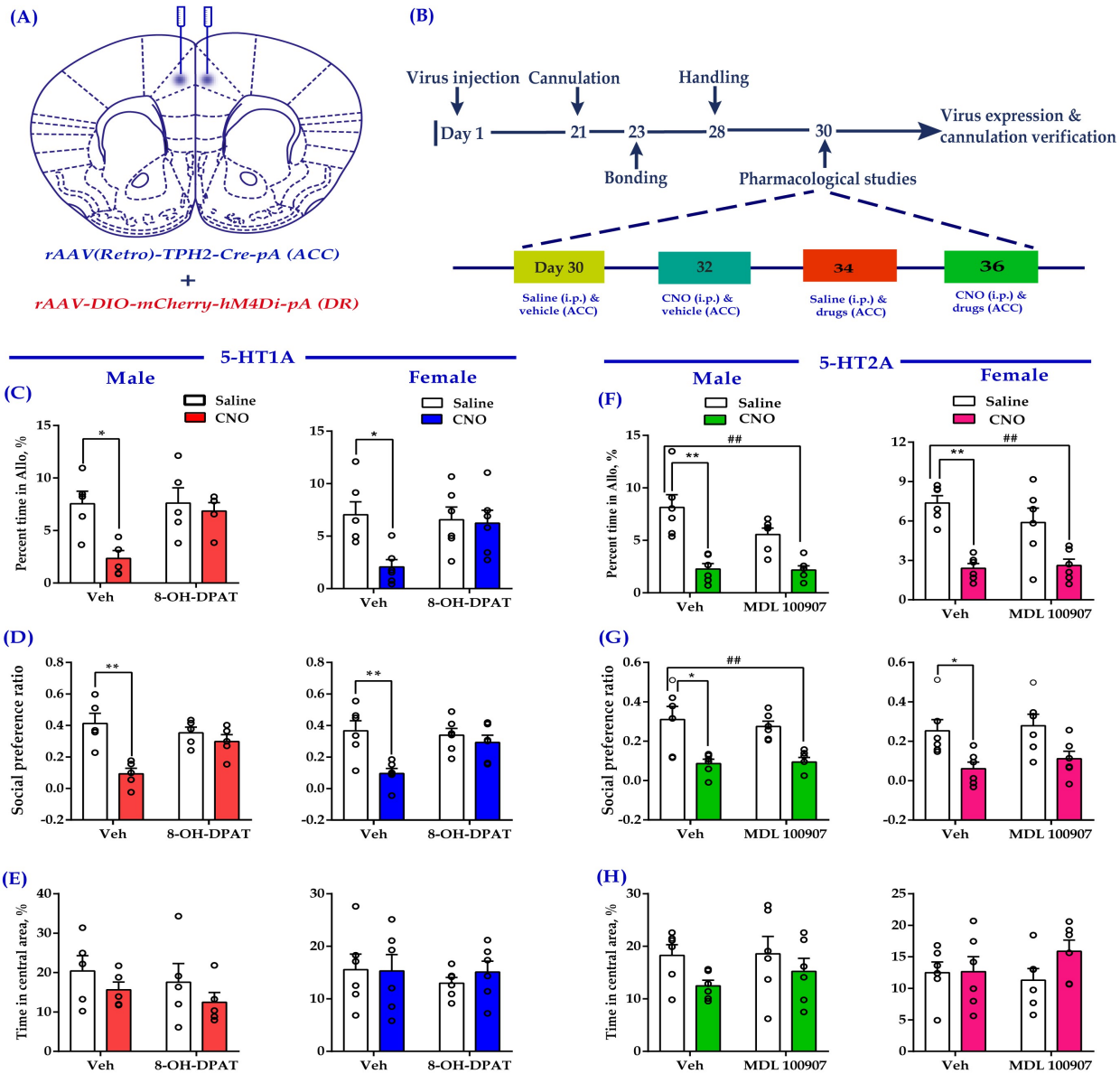

355

356 **Figure 6. Intra-ACC injection of 8-OH-DPAT reduced sociability deficits induced by**

357 **chemogenetic inhibition of DR 5-HT neurons in the DR→ACC neural circuit.** (A): Schematic

358 representation of ACC infusion sites and virus strategy; (B): timeline of experimental design;
359 (C-E): effect of a 5-HT1AR agonist 8-OH-DPAT on allogrooming time in the consolation test (C),
360 social preference ratio in the three-chamber test (D), and time spent in the central area in the
361 open-field test (E) in male (left panels) and female (right panels) voles; (F-H): effect of a 5-HT2AR
362 antagonist (MDL 100907) on allogrooming time in the consolation test (F), social preference ratio
363 in the three-chamber test (G) and time spent in the central area in the open-field test (H) in male
364 (left panels) and female (right panels) voles. Data are presented as mean ± SE, n = 5–6 in each
365 group; two-way ANOVA along with two-way Bayesian ANOVA; *P < 0.05, **P < 0.01 for
366 'vehicle + saline' *vs.* 'vehicle + CNO'; ##P < 0.01 for 'MDL 100907 + CNO' *vs.* 'vehicle + saline'.
367 For raw data in this figure, please refer to Figure 6—source data 1. For detailed quantifications,
368 please refer to Supplementary 2. Anta: antangonist; ACC: anterior cingulate cortex; DR: dorsal
369 raphe nucleus.
370

371 **DISCUSSION**

372 In the present study, we demonstrated a crucial role for the DR→ACC 5-HTergic neural circuit
373 in the regulation of consolation-like behaviors and sociability in mandarin voles for the first time.
374 Our major findings are listed below. First, inhibition of DR 5-HT neurons or their terminals in
375 the ACC decreased allogrooming behavior and reduced sociability. Second, DR 5-HT neuron
376 activity and ACC 5-HT release increased during allogrooming, social approaching and sniffing.
377 Third, direct activation of ACC 5-HT1A receptors was sufficient to ameliorate deficits in
378 consolation and sociability induced by chemogenetic inhibition of DR 5-HT neurons.

379 We found optogenetic inhibition of DR 5-HT neurons (Figure 1) or ACC 5-HT terminals
380 (Figure 2) significantly decreased intimate behaviors (allogrooming and chasing) toward their
381 distressed partners and reduced sociability. Chemogenetic inhibition of DR 5-HT neurons
382 produced similar results (Figure 3). Consistent with our results, Walsh et al found that
383 optogenetic inhibition of DR 5-HT neurons reduced social interactions in the three-chamber test
384 (Walsh et al., 2018). As consolation is in general a pro-social behavior, it is difficult to determine
385 whether the reduced allogrooming is due to an overall decrease in sociability. However, in the
386 fiber photometry studies, we found both DR 5-HT neurons and ACC 5-HT release showed the
387 highest responses during allogrooming, which may indicate the specific role of 5-HT in
388 consolation (Figure 4—figure supplement 2).

389 Another open question is how this process occurs, namely, what are the neural mechanisms
390 underlying this process? The neocortical excitatory/inhibitory (E/I) balance hypothesis may
391 help address this question. The hypothesis indicates that an increase in the cortical cellular E/I
392 balance, for example through increased activity in excitatory neurons or a reduction in inhibitory
393 neuron function, is the common etiology and final pathway for some psychiatric diseases, such
394 as autism and schizophrenia (Bozzi et al., 2018; Vattikuti and Chow, 2010). This hypothesis has
395 recently been verified in mice, as optogenetic excitation of glutamatergic neurons in the mPFC
396 elicits a profound impairment in sociability, while compensatory excitation of inhibitory neurons

397 in this region partially rescues the social deficits caused by an increase in the E/I balance (Yizhar
398 et al., 2011). 5-HT tends to inhibit prefrontal pyramidal activity (Puig and Gulledge, 2011; Tian et
399 al., 2017). For example, according to Puig et al., electrical stimulation of the DR inhibits
400 approximately two-thirds of pyramidal neurons in the mPFC (Puig et al., 2005). Therefore, a
401 reasonable hypothesis is that inhibition of the DR-ACC 5-HTergic neural circuit may increase the
402 E/I balance, which ultimately leads to abnormal social behaviors in mandarin voles. Clearly, this
403 hypothesis should be verified in electrophysiological studies in the future.
404 In contrast to inhibition manipulations, we found activation of the DR-ACC 5-HTergic
405 neural circuit did not elicit corresponding increases in allogrooming and sociability (Figures 1-3).
406 One possible explanation is that there are various 5-HT receptors expressed in the ACC and
407 some have opposite functional effects (Puig and Gulledge, 2011; Tian et al., 2017). For example,
408 5-HT1AR coupled to the Gi family of G proteins induces hyperpolarization of pyramidal
409 neurons, whereas 5-HT2AR coupled to Gq proteins induces depolarization in the same neurons
410 (Carhart-Harris and Nutt, 2017). In addition, these two types of receptors are expressed in both
411 pyramidal and GABAergic neurons of the mPFC (Santana et al., 2004). Therefore, the net
412 behavioral effects of 5-HT release must result from the combined effects of all these receptors.
413 The other possible explanation is a ceiling effect, which means that the enhancement of
414 consolation and sociability are difficult to accomplish in these normal animals. This may occur in
415 situations where levels of consolation and sociability are low such as in the stressed subjects in
416 our previous study (Li et al., 2020) or genetically less sociable subjects as in Walsh's study (Walsh
417 et al., 2018). However, in a previous study by Kim et al., the direct administration of 5-HT into
418 the ACC impaired observational fear learning, which is an indicator of emotional contagion (Kim
419 et al., 2014). Species differences (mice *vs.* voles), methodological differences (pharmacology *vs.*
420 optogenetics and chemogenetics) or different behavioral indicators (consolation *vs.* emotional
421 contagion) may account for the discrepancies. Furthermore, optogenetic or chemogenetic
422 activation of DR 5-HT neurons is also distinct from pharmacological intervention with MDMA,
423 which robustly induces 5-HT releases in the whole brain and enhances closeness and empathy in

424 its users in human studies (Carlyle et al., 2019; Heifets and Malenka, 2016). Nevertheless, at least
425 some effects of activation were visible. For example, optogenetic activation of ACC 5-HT
426 terminals increased sociability in CHR2-expressing females (Figure 2E). Clearly, the effects of
427 activation of the DR-ACC 5-HTergic neural circuit on sociability and empathy still require
428 further in-depth study.

429 Our results show that neither activation nor inhibition the DR-ACC 5-HTergic neural circuit
430 exerts any significant effects on some control behaviors (Figure 1—figure supplement 4; Figure
431 2—figure supplement 1; Figure 3—figure supplement 2), i.e., self-grooming in the consolation
432 test or behavioral performance in the open-field test, which is consistent with pervious results
433 (for self-grooming, please refer to (Correia et al., 2017); for the open-field test, please refer to
434 (Walsh et al., 2018)). However, inconsistent results have also been reported. For example,
435 Ohmura et al. found that optogenetic activation of 5-HT neurons in the median raphe nucleus
436 enhanced anxiety-like behaviors in mice (Ohmura et al., 2014). In the study by Correia et al.,
437 activation of 5-HTergic neurons in the DR affected behavior in the open-field test, but not anxiety
438 (Correia et al., 2017). Different stimulation protocols or manipulations of different groups of
439 5-HT neurons may account for these discrepancies.

440 Our results obtained using *in vivo* fiber photometry indicated an increase in DR 5-HT
441 neuron activity during allogrooming, sniffing and social approaching (Figure 4). This result is
442 consistent with previous studies showing increases in the activity of 5-HTergic neurons in the
443 DR during nonaggressive social interactions (Li et al., 2016; Walsh et al., 2018). Furthermore,
444 using the highly sensitive 5-HT fluorescent sensors developed by Wan et al., (Wan et al, 2020),
445 we provided the first evidence that allogrooming, sniffing and social approaching elicit robust
446 5-HT release in the ACC (Figure 5). Self-grooming and running did not induce robust 5-HT
447 release within the ACC, which may indicate the behavioral relevance of the 5-HT sensors.
448 Interestingly, we found that the fluorescence changes in GCamP6 and 5-HT sensors usually
449 precede allogrooming and social approaching and decreased accordingly before withdrawing
450 from them (Figure 4—figure supplement 3, Figure 5—figure supplement 1). These results

451 indicate that 5-HT may be involved in some motivational aspects of these social behaviors, which
452 is consistent with previous findings (Arakawa, 2020; Yagishita, 2020).
453 Although both 5-HT1AR and 5-HT2AR are expressed at high levels in the mPFC and work
454 together to modulate cortical network activity (Celada et al., 2013), we found only the 5-HT1AR
455 receptor agonist significantly reduced the consolation and sociability deficits induced by
456 chemogenetic inhibition of 5-HTergic neurons in the DR (Figure 6). This result is consistent with
457 our previous finding that the administration of WAY-100635 (a 5-HT1AR antagonist) into the
458 ACC attenuates consolation and sociability in mandarin voles (Li et al., 2020). 5-HT1AR within
459 the mPFC has frequently been reported to exert antidepressant and anxiolytic effects (Artigas,
460 2013; Fukumoto et al., 2020; Fukumoto et al., 2014; Wang et al., 2019), but our findings clearly
461 indicate that this type of 5-HT receptor within the ACC is also involved in regulating some social
462 behaviors. Clearly, this effect should be verified in many other species in future studies.
463 Administration of the 5-HT2AR antagonist into the ACC did not exert an obvious effect on the
464 social deficits induced by the chemogenetic inhibition of DR 5-HT neurons (Figure 5F-H). Thus,
465 5-HT2AR within the ACC may not play a major role in consolation and sociability. However,
466 this conclusion should be interpreted very cautiously because 5-HT2AR expression within the
467 mPFC shows clear rostral-to-caudal gradients in mice (Weber and Andrade, 2010) and we were
468 unable to determine its functional role in this dimension in the present study. Furthermore, the
469 effects of 5-HT in the ACC on consolation and sociability probably involve other subtypes of
470 5-HT receptors, such as 5-HT1BR and 5-HT3R, which require further examination.
471 In conclusion, our findings establish the importance of the DR-ACC 5-HTergic neural circuit
472 in consolation-like behaviors and sociability in mandarin voles. One major limitation of our
473 study is that although our virus strategies were generally successful, a few of the infected
474 neurons were indeed TPH2-negative, which may challenge the specificity of our manipulations
475 and confound our results. However, the fiber photometry and pharmacological studies mitigate
476 these concerns. Considering the widespread innervation of 5-HT terminals and abundant
477 distribution of 5-HT receptors in the whole brain, detailed knowledge of cellular and circuit

478 mechanisms of the 5-HTergic system, will not only improve our understanding of its
479 complicated features and functions but also have implications for the development of novel
480 therapies for the treatment of prevalent neuropsychiatric disorders, such as depression, autism,
481 and schizophrenia. Additionally, although both male and female subjects were included in this
482 study, sexually dimorphic effects were rarely observed. This finding may provide additional
483 evidence of cooperative evolution to adapt to environmental challenges, particularly in species
484 that adapt monogamous relationships and require cooperative breeding.

485

486

487

488

489

490

491

492

493

494

495

496

497 **METHODS AND MATERIALS**

498 **Key Resources Table**

Reagent type	Source	Identifier	Additional information
Antibodies			
Anti-TPH2 goat polyclonal antibody	Abcam	ab121013	1/500
Donkey anti-goat secondary antibody conjugated with Dylight 488	Jackson	705-545-147	1/300
Donkey anti-goat secondary antibody conjugated with TRITC	Jackson	705-025-003	1/300
DAPI	Boster	AR1177	Original fluid
Drugs and compounds			
8-OH-DPAT	Sigma	H8520	Injection site : ACC; volume: 200 nL/side; concentration: 1.5 mg/mL
MDL 100907	Tocris Bioscience	Cat#4173	Injection site : ACC; volume: 200 nL/side; concentration: 1 mg/mL
Metergoline	MedChem Express	Cat#HY-B1033/CS-4551	4mg/kg, i.p.
CNO	BrainVTA	Cat# CNO-02	1 mg/kg, i.p.
Cholera Toxin Subunit B (CTB)594	Thermo Fisher	Cat#C34777	Injection site : ACC ; volume : 400 nL/side ; expression time : 10 days
Optogenetic virus			
rAAV(Retro)-TPH2-Cre-WPRE-pA	BrainVTA	R-396-K181127	Injection site : ACC ; volume : 300 nL/side ; expression time : 5 wks
rAAV-Ef1α-DIO-ChR2-mC	BrainVTA	9-2-K190827	Injection site : DR;

herry-WPRE-pA			volume : 500 nL ; expression time : 5 wks
rAAV-Ef1α-DIO-eNpHR3.0-mCherry-WPRE-pA	BrainVTA	rAAV9-7-5-1	Injection site : DR; volume : 500 nL ; expression time : 5 wks
rAAV-Ef1α-DIO-mCherry-WPRE-pA	BrainVTA	9-13-K190430	Injection site : DR; volume : 500 nL ; expression time : 5 wks
Chemogenetic virus			
rAAV(Retro)-TPH2-Cre-WPRE-pA	BrainVTA	R-396-K181127	Injection site : ACC ; volume : 300 nL/side ; expression time : 5 wks
rAAV-Ef1α-DIO-hM4Di(Gi)-mCherry-WPRE-pA	BrainVTA	9-43-K190521	Injection site : DR; volume : 500 nL ; expression time : 5 wks
rAAV-Ef1α-DIO-hM4Dq(Gq)-mCherry-WPRE-pA	BrainVTA	9-42-K190530	Injection site : DR; volume : 500 nL ; expression time : 5 wks
Fiber photometry virus			
rAAV-hSyn-5HT2.1-WPRE-hGHpA (5-HT sensor)	BrainVTA	9-1826-K190620	Injection site : ACC ; volume : 400 Nl ; expression time : 3 wks
rAAV-hSyn-EGFP-WPRE-hGH-pA	BrainVTA	PT-1990	Injection site : ACC ; volume : 400 nL; expression time : 3 wks
rAAV-EF1α-DIO-GCaMp6-WPRE-hGH pA	BrainVTA	PT-0071	Injection site : DR; volume : 500 nL ; expression time : 4 wks
rAAV-hSyn-DIO-EGFP-WPRE-hGH-PA	BrainVTA	9-1103-K200409	Injection site : DR; volume : 500 nL; expression time : 4 wks
rAAV(Retro)-TPH2-Cre-WPRE-pA	BrainVTA	R-396-K181127	Injection site : ACC ; volume : 300 nL/side ; expression time : 4 wks

499 **Animals**

500 The mandarin voles used in this study were laboratory bred strains (F2-F3) whose ancestors
501 derived from a wild population from Lingbao city (Henan, China). The voles were weaned on
502 postnatal day 21, socially housed in same-sex in each polycarbonate cage (44×22×16 cm) and
503 housed on a 12-h light/dark cycle with food and water ad libitum. Voles used for experiments
504 were about 70-90 days old at the time. All breeding, housing, and experimental procedures were
505 in accordance with Chinese guidelines for the care and use of laboratory animals and were
506 approved by the Animal Care and Use Committee of Shaanxi Normal University.

507 **Stereotaxic surgery and virus infusions**

508 The kind of virus, total injection volumes and the expression time were listed in Key Resources
509 Table. For surgery, voles (about 50 days) were anesthetized with 1.5%-3.0% isoflurane and
510 placed in a stereotaxic instrument. Next, thirty-three-gauge syringe needles (Hamilton) were
511 used for virus delivery. The injection rates were set at 50 nL/min. After each injection, the needle
512 was left in the brain for another 5 min before being slowly withdrawn in order to prevent the
513 virus from leaking out. The bregma coordinates for the virus injection were as follows: ACC:
514 A/P: 1.6, M/L: 0.5, D/V: 1.6; DR: AP: -4.3; DV: -3.3, ML: +1.2, with a 20 angle toward the midline
515 in the coronal plane.

516 **Microinjection and drugs**

517 The 5-HT1AR agonist 8-OH-DPAT was prepared in saline with a final concentration of 1.5
518 mg/mL. The 5-HT2AR antagonist MDL 100907 was prepared in 0.01 M PBS (adjust PH value
519 with 0.1 M HCl to 6.4) with a final concentration of 1 mg/mL. All the microinjections were
520 administered 30 min before the behavioral test. The speed of injection was 0.1 μL/min, and the
521 total injection volume were 0.2 μL per side for all the drugs. The injector tips remained in situ for
522 another 2 min for drug diffusions. The dose and timing of drug administration were chosen
523 based on previous studies with 8-OH-DPAT (Cooper et al., 2008; Li et al., 2020) and MDL 100907

524 (Ishii et al., 2015; Pockros et al., 2011), which adjusted according to preliminary studies. In
525 chemogenetic studies, CNO (1 mg/kg) was dissolved in saline and delivered intraperitoneally 30
526 min before the behavioral test.

527 **Optogenetic studies**

528 For optogenetic activation, ferrules were connected (by patch cords) to a 473 nm laser diode
529 through a FC/PC adaptor and a fiber optic rotary joint. The output parameters were: 10 ms, 20
530 Hz, 8 s on and 2 s off cycle, ～10 mW for terminal stimulation, ～5 mW for somatic stimulation.
531 For optogenetic inhibition, ferrules were connected to a 593 nm laser diode. The output
532 parameters were: 10 ms, 20 Hz, constant, ～10 mW for both terminal and somatic inhibition. The
533 optogenetic stimulation parameters were chosen and slightly modified based on previous
534 studies (Garcia-Garcia et al., 2018; Walsh et al., 2018; Zhao et al., 2011)

535 **Behavioral assays**

536 Generally, all the behavioral experiments were performed under dim light during the dark phase
537 of the light-dark cycle. In all tests, all groups of experimental voles were randomly selected and
538 the observers were blinded to the treatments. During the test, if the subject (not the stimulus
539 voles) showed very rare or no movements, we think these individuals did not show normal
540 activity, and their data are not appropriate to include in the following analysis. For optogenetic
541 and fiber photometry studies, all subjects were allowed to habituate to patch cords for at least
542 three days and allowed 30 min acclimation to the connection before the experiment started.

543 <u>Consolation test</u>

544 The consolation test was performed as previously described (Burkett et al., 2016). Briefly, five
545 days before the experiment, age-matched adult male and female voles were cohoused together to
546 promote the formation of a pair bond (Yu et al., 2012). On the testing day, the subjects' partners
547 were gently transferred in a cup to a sound-proof electric shock chamber and then subjected to

548 10 rounds of moderately strong foot shocks (3 s, 0.8 mA, 2 min intertrial intervals). At the same
549 time, the test voles were left undisturbed in their home cages. After the separation, the pairs
550 were reunited, and the behavior of the subjects was recorded using a video camera for 10 min in
551 the test room. The digital videos were viewed and quantified using J Watcher software
552 (http://www.jwatcher.ucla.edu/). According to previous studies (Burkett et al., 2016; Li et al.,
553 2019), allogrooming is designated as behavioral indicators of consolation, which defined as head
554 contact with the body or head of their partner, accompanied by a rhythmic head movement. The
555 duration of chasing (following the shocked partners) and selfgrooming were also collected and
556 analyzed.

557 For optogenetic tests, it designed as a between-subjects test in which both groups (mCherry
558 or opsin) received laser stimulation. The lasting effects of optogenetic inhibition were measured
559 24 h after the original test, i.e., consolation test was conducted once again without light
560 stimulation in eNPHR 3.0 animals one day later.

561 Three-chamber test

562 The three-chamber test was used to assess the sociability of a subject (Horie et al., 2019; Walsh et
563 al., 2018). The apparatus consisted of a rectangular box with three separate chambers (20 × 40 ×
564 20 cm each). One side of each chamber contained a circular metal wire cage (stimulus animal
565 cage, 11 cm high and 9 cm in diameter). One day before the test, all subjects were habituated to
566 the arena for 5 min and an age- and sex-matched unfamiliar stimulus voles also habituated to the
567 wire cages for 5 min. On the testing day, the test vole was placed in the center chamber and a
568 'stimulus' vole (housed in a same room with the test voles) was randomly placed into one of the
569 wire cages. After 2 min, the partitioning walls between the chambers were removed and the test

570 voles were allowed to explore freely for a 10 min session. The time spent exploring each chamber
571 was automatically recorded using a video tracking system (Shanghai Xinruan, China). Sociability
572 was calculated as follows: (time spent in the stimulus vole side − time spent in the empty
573 side)/(time spent in the stimulus vole side + time spent in the empty side).
574 For optogenetic tests, voles received four epochs of light beginning with a light OFF baseline
575 epoch (OFF-ON-OFF-ON). Each epoch lasted for 5 min and the total duration was 20 min.

576 Open-field test

577 The anxiety level and locomotor function of the subjects were assessed by using the open-field
578 test (Flanigan et al., 2020; Walsh et al., 2018). Briefly, a square open field (50 cm × 50 cm × 25 cm)
579 was virtually subdivided into 16 even square. The four central squares were designated as
580 central area. At the beginning of the test, the test vole was placed into the center area facing
581 away from the experimenter. Behavior was recorded for 5 min. Outcome measures were distance
582 traveled, frequency entries and time spent in the central area.
583 For optogenetic tests, voles were tested twice in the same day in both light-off and light-on
584 conditions with at least 2 h between sessions (within-subjects design).

585 **Fiber photometry**

586 The fiber photometry recording set-up (ThinkerTech, Nanjing, China) was generated and used as
587 previously described (Feng et al., 2019; Yuan et al., 2019). Briefly, the emission light was
588 generated by a 480 LED, reflected with a dichroic mirror and delivered to the brain in order to
589 excite the GCaMP6m or the 5-HT sensor. The emission light passed through another band pass
590 filter, into a CMOS detector (Thorlabs, Inc. DCC3240M) and finally recorded by a Labview
591 program (TDMSViewer, ThinkerTech, Nanjing, China).
592 On the test day, voles were mildly anesthetized with isoflurane and connected to a

593 muti-mode optic fiber patch cord (ThinkerTech Nanjing Bioscience®, NA: 0.37, OD: 200 μm)
594 which the other end connected to fiber photometry apparatus. After 30 min habituation, the
595 voles were subjected to consolation test as described above (exposure to their shocked partners)
596 and the behavioral recording consisted of allogrooming, sniffing, social approaching,
597 self-grooming and running. During the test, if a specific behavior occurred no more than four
598 times within 1 h, the record was replicated in the following day.
599 Fiber photometry signals were processed with custom-written MATLAB software. Briefly,
600 all the data were segmented based on the behavioral events and baseline phase. The change in
601 fluorescence (ΔF/F) was calculated as (F–F0)/F0, where F0 represents the baseline fluorescence
602 signal averaged over a 10 s-long control time window. We first segmented the data based on the
603 behavioral events. Then, we calculated the average 5-HT and calcium signals in both the pre-
604 and post-phases (2/8 s). The time window was determined according to the duration of a
605 behavior bout. The response elicited during a behavior was calculated as the average ΔF/F
606 during all trials of a particular behavior. The peak response during a behavior was calculated as
607 the maximum ΔF/F during the behavior minus F0.
608 For specificity verification of 5-HT sensors in Figure 5—figure supplement 2, a 5-HT
609 receptor antagonist metergoline (Met) was injected (i.p., 4 mg/kg) 20 min before the fiber
610 photometry experiments. The timing and dosing were chosen according to previous studies
611 (Onasanwo et al., 2016; Wan, et al 2020).

612 ***In vitro* electrophysiological recordings**

613 To verify the optogenetic and chemogenetic manipulations, we performed *in vitro* whole-cell
614 patch-clamp recordings from DR neurons. Neurons expressing ChR2, eNpHR3.0, hM3Dq and
615 hM4Di were visually identified by fluorescence of mCherry. The voles were anesthetized with
616 isoflurane. Brains were quickly dissected and 300 μm coronal slices containing the DRN were
617 prepared in a chamber filled with ACSF (32-34℃) using vibratome (Campden 7000 smz). The
618 recordings were obtained using a Multiclamp 700B amplifier, filtered at 5 kHz and sampled at 10

619 kHz with Digidata 1440A. Clampex 10.5 was used for analysis.

620 Current-clamp recordings were performed to measure evoked action potentials. For
621 photoactivation and photoinhibition, the light protocols used during behavioral tests were
622 delivered through a 200 μm optical fiber close to recorded neurons. For CNO activation,
623 spontaneous firing of action potentials in the cell was recorded in current clamp mode at -60 mV.
624 After 5 min of recording, the slices were perfused with 10 μM CNO. The total recording time for
625 each cell was 10 min. For CNO inhibition, we applied currents in steps of 25 pA, ranging from 0
626 pA to 250 pA. Neurons were allowed to recover for 10 min then perfused with 10 μM CNO. The
627 same current procedure was performed. Afterwards, the CNO was removed by washes with
628 ASCF and cells were recorded for another 10 min.

629 **Data analysis**

630 All data are represented as the mean ± SE. All data were assessed for normality using a
631 one-sample Kolmogorov-Smirnov test, and the Levene's test was used to confirm homogeneity
632 of variance. Comparisons between two groups were performed by unpaired or paired *t* tests.
633 Comparisons among three or more groups of different animals were performed
634 using one-way ANOVA. Two-way ANOVAs or two-way repeated measures ANOVAs were
635 used to compare multiple groups under multiple testing conditions when appropriate. Post hoc
636 comparisons were conducted using Tukey. To confirm the significance and calculate the effect
637 size, Bayesian *t* test (paired or unpaired) and Bayesian ANOVA were conducted for all the
638 comparisons using default priors. For more detailed information about the Bayesian test, please
639 refer to Dr. Keysers's work (Keysers et al., 2020). The data were analyzed using JASP 14.0 and are
640 presented as the mean ± SE. The significant level was set at $P < 0.05$. The detailed analysis
641 method in each figure and the statistical quantifications are presented in Supplementary 2.

642

643

644

ACKNOWLEDGMENTS AND DISCLOSURES

This research was supported by the National Natural Science Foundation of China (31970424, 31670421, 31372213 and 31772473), the Natural Science Basic Research Plan in Shaanxin Province of China (2018JM3032) and the Fundamental Research Funds for Central University (GK201903059). We thank Yu-Ying Yang, Xin Zhang and Yi-Xin Feng for assistance in conducting experiments and caring for voles. The authors declare no conflict of interest.

AUTHOR CONTRIBUTIONS

Prof. F.D.T. designed the study; L.F.L. conducted the majorities of experiments and wrote the original draft; L.Z.Z participated in the electrophysiological experiment; Z.X.H. and R.J. discussed the results and provided constructive comments; Y.T.Z participated in the fiber photometry studies. H.M., Y.F.X, W.Y., W.J.H., Z.J.L. and L.Y.T. participated in the behavior study and helped to collect and analyze the data. All authors contributed to and have approved the final manuscript.

APPENDIX

Supplementary 1. Supplemental figures.

Supplementary 2. Analysis methods and the statistical quantifications

665 **REFERENCE**

666 Arakawa, H., 2020. Somatosensorimotor and Odor Modification, Along with Serotonergic
667 Processes Underlying the Social Deficits in BTBR T+ Itpr3(tf)/J and BALB/cJ Mouse
668 Models of Autism. Neuroscience 445, 144-162.

669 Artigas, F., 2013. Serotonin receptors involved in antidepressant effects. Pharmacology &
670 therapeutics 137, 119-131.

671 Bozzi, Y., Provenzano, G., Casarosa, S., 2018. Neurobiological bases of autism-epilepsy
672 comorbidity: a focus on excitation/inhibition imbalance. The European journal of
673 neuroscience 47, 534-548.

674 Burkett, J.P., Andari, E., Johnson, Z.V., Curry, D.C., de Waal, F.B., Young, L.J., 2016.
675 Oxytocin-dependent consolation behavior in rodents. Science (New York, N.Y.) 351,
676 375-378.

677 Carhart-Harris, R.L., Nutt, D.J., 2017. Serotonin and brain function: a tale of two receptors.
678 Journal of psychopharmacology (Oxford, England) 31, 1091-1120.

679 Carlyle, M., Stevens, T., Fawaz, L., Marsh, B., Kosmider, S., Morgan, C.J., 2019. Greater empathy
680 in MDMA users. Journal of psychopharmacology (Oxford, England) 33, 295-304.

681 Celada, P., Puig, M.V., Artigas, F., 2013. Serotonin modulation of cortical neurons and networks.
682 Frontiers in integrative neuroscience 7, 25.

683 Charnay, Y., Leger, L., 2010. Brain serotonergic circuitries. Dialogues in clinical neuroscience 12,
684 471-487.

685 Cooper, M.A., McIntyre, K.E., Huhman, K.L., 2008. Activation of 5-HT1A autoreceptors in the
686 dorsal raphe nucleus reduces the behavioral consequences of social defeat.

687 Psychoneuroendocrinology 33, 1236-1247.

688 Correia, P.A., Lottem, E., Banerjee, D., Machado, A.S., Carey, M.R., Mainen, Z.F., 2017. Transient
689 inhibition and long-term facilitation of locomotion by phasic optogenetic activation of
690 serotonin neurons. eLife 6.

691 de Waal, F.B., 2008. Putting the altruism back into altruism: the evolution of empathy. Annual
692 review of psychology 59, 279-300.

693 de Waal, F.B.M., Preston, S.D., 2017. Mammalian empathy: behavioural manifestations and
694 neural basis. Nature reviews. Neuroscience 18, 498-509.

695 Dolder, P.C., Grunblatt, E., Muller, F., Borgwardt, S.J., Liechti, M.E., 2017. A Single Dose of LSD
696 Does Not Alter Gene Expression of the Serotonin 2A Receptor Gene (HTR2A) or Early
697 Growth Response Genes (EGR1-3) in Healthy Subjects. Frontiers in pharmacology 8, 423.

698 Dolen, G., Darvishzadeh, A., Huang, K.W., Malenka, R.C., 2013. Social reward requires
699 coordinated activity of nucleus accumbens oxytocin and serotonin. Nature 501, 179-184.

700 Faye, C., Hen, R., Guiard, B.P., Denny, C.A., Gardier, A.M., Mendez-David, I., David, D.J., 2020.
701 Rapid Anxiolytic Effects of RS67333, a Serotonin Type 4 Receptor Agonist, and Diazepam,
702 a Benzodiazepine, Are Mediated by Projections From the Prefrontal Cortex to the Dorsal
703 Raphe Nucleus. Biological psychiatry 87, 514-525.

704 Feng, J., Zhang, C., Lischinsky, J.E., Jing, M., Zhou, J., Wang, H., Zhang, Y., Dong, A., Wu, Z., Wu,
705 H., Chen, W., Zhang, P., Zou, J., Hires, S.A., Zhu, J.J., Cui, G., Lin, D., Du, J., Li, Y., 2019.
706 A Genetically Encoded Fluorescent Sensor for Rapid and Specific In Vivo Detection of
707 Norepinephrine. Neuron 102, 745-761 e748.

708 Field, T., Diego, M., Hernandez-Reif, M., 2009. Depressed mothers' infants are less responsive to

709 faces and voices. Infant behavior & development 32, 239-244.

710 Flanigan, M.E., Aleyasin, H., Li, L., Burnett, C.J., Chan, K.L., LeClair, K.B., Lucas, E.K.,
711 Matikainen-Ankney, B., Durand-de Cuttoli, R., Takahashi, A., Menard, C., Pfau, M.L.,
712 Golden, S.A., Bouchard, S., Calipari, E.S., Nestler, E.J., DiLeone, R.J., Yamanaka, A.,
713 Huntley, G.W., Clem, R.L., Russo, S.J., 2020. Orexin signaling in GABAergic lateral
714 habenula neurons modulates aggressive behavior in male mice. Nature neuroscience.

715 Fu, W., Le Maitre, E., Fabre, V., Bernard, J.F., David Xu, Z.Q., Hokfelt, T., 2010. Chemical
716 neuroanatomy of the dorsal raphe nucleus and adjacent structures of the mouse brain.
717 The Journal of comparative neurology 518, 3464-3494.

718 Fukumoto, K., Fogaça, M.V., Liu, R.J., Duman, C.H., Li, X.Y., Chaki, S., Duman, R.S., 2020.
719 Medial PFC AMPA receptor and BDNF signaling are required for the rapid and
720 sustained antidepressant-like effects of 5-HT(1A) receptor stimulation.
721 Neuropsychopharmacology : official publication of the American College of
722 Neuropsychopharmacology 45, 1725-1734.

723 Fukumoto, K., Iijima, M., Chaki, S., 2014. Serotonin-1A receptor stimulation mediates effects of a
724 metabotropic glutamate 2/3 receptor antagonist,
725 2S-2-amino-2-(1S,2S-2-carboxycycloprop-1-yl)-3-(xanth-9-yl)propanoic acid (LY341495),
726 and an N-methyl-D-aspartate receptor antagonist, ketamine, in the novelty-suppressed
727 feeding test. Psychopharmacology 231, 2291-2298.

728 Garcia-Garcia, A.L., Canetta, S., Stujenske, J.M., Burghardt, N.S., Ansorge, M.S., Dranovsky, A.,
729 Leonardo, E.D., 2018. Serotonin inputs to the dorsal BNST modulate anxiety in a 5-HT1A
730 receptor-dependent manner. Molecular psychiatry 23, 1990-1997.

731 Gong, P., Liu, J., Blue, P.R., Li, S., Zhou, X., 2015. Serotonin receptor gene (HTR2A) T102C
732 polymorphism modulates individuals' perspective taking ability and autistic-like traits.
733 Frontiers in human neuroscience 9, 575.
734 Gyurak, A., Haase, C.M., Sze, J., Goodkind, M.S., Coppola, G., Lane, J., Miller, B.L., Levenson,
735 R.W., 2013. The effect of the serotonin transporter polymorphism (5-HTTLPR) on
736 empathic and self-conscious emotional reactivity. Emotion (Washington, D.C.) 13, 25-35.
737 Heifets, B.D., Malenka, R.C., 2016. MDMA as a Probe and Treatment for Social Behaviors. Cell
738 166, 269-272.
739 Horie, K., Inoue, K., Suzuki, S., Adachi, S., Yada, S., Hirayama, T., Hidema, S., Young, L.J.,
740 Nishimori, K., 2019. Oxytocin receptor knockout prairie voles generated by
741 CRISPR/Cas9 editing show reduced preference for social novelty and exaggerated
742 repetitive behaviors. Hormones and behavior 111, 60-69.
743 Ishii, H., Ohara, S., Tobler, P.N., Tsutsui, K., Iijima, T., 2015. Dopaminergic and serotonergic
744 modulation of anterior insular and orbitofrontal cortex function in risky decision making.
745 Neuroscience research 92, 53-61.
746 Keysers, C., Gazzola, V., Wagenmakers, E.J., 2020. Using Bayes factor hypothesis testing in
747 neuroscience to establish evidence of absence. Nature neuroscience 23, 788-799.
748 Kim, B.S., Lee, J., Bang, M., Seo, B.A., Khalid, A., Jung, M.W., Jeon, D., 2014. Differential
749 regulation of observational fear and neural oscillations by serotonin and dopamine in the
750 mouse anterior cingulate cortex. Psychopharmacology 231, 4371-4381.
751 Knapska, E., Mikosz, M., Werka, T., Maren, S., 2010. Social modulation of learning in rats.
752 Learning & memory (Cold Spring Harbor, N.Y.) 17, 35-42.

753 Li, L.F., Yuan, W., He, Z.X., Ma, H., Xun, Y.F., Meng, L.R., Zhu, S.J., Wang, L.M., Zhang, J., Cai,
754 W.Q., Zhang, X.N., Guo, Q.Q., Lian, Z.M., Jia, R., Tai, F.D., 2020. Reduced Consolation
755 Behaviors in Physically Stressed Mandarin Voles: Involvement of Oxytocin, Dopamine
756 D2, and Serotonin 1A Receptors Within the Anterior Cingulate Cortex. The international
757 journal of neuropsychopharmacology 23, 511-523.
758 Li, L.F., Yuan, W., He, Z.X., Wang, L.M., Jing, X.Y., Zhang, J., Yang, Y., Guo, Q.Q., Zhang, X.N.,
759 Cai, W.Q., Hou, W.J., Jia, R., Tai, F.D., 2019. Involvement of oxytocin and GABA in
760 consolation behavior elicited by socially defeated individuals in mandarin voles.
761 Psychoneuroendocrinology 103, 14-24.
762 Li, Y., Zhong, W., Wang, D., Feng, Q., Liu, Z., Zhou, J., Jia, C., Hu, F., Zeng, J., Guo, Q., Fu, L.,
763 Luo, M., 2016. Serotonin neurons in the dorsal raphe nucleus encode reward signals.
764 Nature communications 7, 10503.
765 Luo, M., Zhou, J., Liu, Z., 2015. Reward processing by the dorsal raphe nucleus: 5-HT and
766 beyond. Learning & memory (Cold Spring Harbor, N.Y.) 22, 452-460.
767 Matsunaga, M., Ishii, K., Ohtsubo, Y., Noguchi, Y., Ochi, M., Yamasue, H., 2017. Association
768 between salivary serotonin and the social sharing of happiness. PloS one 12, e0180391.
769 Meneses, A., Liy-Salmeron, G., 2012. Serotonin and emotion, learning and memory. Reviews in
770 the neurosciences 23, 543-553.
771 Ohmura, Y., Tanaka, K.F., Tsunematsu, T., Yamanaka, A., Yoshioka, M., 2014. Optogenetic
772 activation of serotonergic neurons enhances anxiety-like behaviour in mice. The
773 international journal of neuropsychopharmacology 17, 1777-1783.
774 Onasanwo, S.A., Faborode, S.O., Ilenre, K.O., 2016. Antidepressant-like Potentials of Buchholzia

775 Coriacea Seed Extract: Involvement of Monoaminergic and Cholinergic Systems, and
776 Neuronal Density in the Hippocampus of Adult Mice. Nigerian journal of physiological
777 sciences : official publication of the Physiological Society of Nigeria 31, 93-99.
778 Perez-Manrique, A., Gomila, A., 2018. The comparative study of empathy: sympathetic concern
779 and empathic perspective-taking in non-human animals. Biological reviews of the
780 Cambridge Philosophical Society 93, 248-269.
781 Pockros, L.A., Pentkowski, N.S., Swinford, S.E., Neisewander, J.L., 2011. Blockade of 5-HT2A
782 receptors in the medial prefrontal cortex attenuates reinstatement of cue-elicited
783 cocaine-seeking behavior in rats. Psychopharmacology 213, 307-320.
784 Puig, M.V., Artigas, F., Celada, P., 2005. Modulation of the activity of pyramidal neurons in rat
785 prefrontal cortex by raphe stimulation in vivo: involvement of serotonin and GABA.
786 Cerebral cortex (New York, N.Y. : 1991) 15, 1-14.
787 Puig, M.V., Gulledge, A.T., 2011. Serotonin and prefrontal cortex function: neurons, networks,
788 and circuits. Molecular neurobiology 44, 449-464.
789 Santana, N., Artigas, F., 2017. Laminar and Cellular Distribution of Monoamine Receptors in Rat
790 Medial Prefrontal Cortex. Frontiers in neuroanatomy 11, 87.
791 Santana, N., Bortolozzi, A., Serrats, J., Mengod, G., Artigas, F., 2004. Expression of serotonin1A
792 and serotonin2A receptors in pyramidal and GABAergic neurons of the rat prefrontal
793 cortex. Cerebral cortex (New York, N.Y. : 1991) 14, 1100-1109.
794 Tian, Z., Yamanaka, M., Bernabucci, M., Zhao, M.G., Zhuo, M., 2017. Characterization of
795 serotonin-induced inhibition of excitatory synaptic transmission in the anterior cingulate
796 cortex. Molecular brain 10, 21.

797 Vattikuti, S., Chow, C.C., 2010. A computational model for cerebral cortical dysfunction in
798 autism spectrum disorders. Biological psychiatry 67, 672-678.
799 Walsh, J.J., Christoffel, D.J., Heifets, B.D., Ben-Dor, G.A., Selimbeyoglu, A., Hung, L.W.,
800 Deisseroth, K., Malenka, R.C., 2018. 5-HT release in nucleus accumbens rescues social
801 deficits in mouse autism model. Nature 560, 589-594.
802 Wan JX, Peng WL, Li XL, Qian TG, Song K, Zeng JZ, et al. A genetically encoded GRAB sensor
803 for measuring serotonin dynamics in vivo. *Biorxiv*. 2020; 38:569-580; posted February 25,
804 2020; doi: 10.1101/2020.02.24.962282.
805 Wang, L., Zhu, Z., Hou, W., Zhang, X., He, Z., Yuan, W., Yang, Y., Zhang, S., Jia, R., Tai, F., 2019.
806 Serotonin Signaling Trough Prelimbic 5-HT1A Receptors Modulates CSDS-Induced
807 Behavioral Changes in Adult Female Voles. The international journal of
808 neuropsychopharmacology 22, 208-220.
809 Weber, E.T., Andrade, R., 2010. Htr2a Gene and 5-HT(2A) Receptor Expression in the Cerebral
810 Cortex Studied Using Genetically Modified Mice. Frontiers in neuroscience 4.
811 Yagishita, S., 2020. Transient and sustained effects of dopamine and serotonin signaling in
812 motivation-related behavior. Psychiatry and clinical neurosciences 74, 91-98.
813 Yizhar, O., Fenno, L.E., Prigge, M., Schneider, F., Davidson, T.J., O'Shea, D.J., Sohal, V.S., Goshen,
814 I., Finkelstein, J., Paz, J.T., Stehfest, K., Fudim, R., Ramakrishnan, C., Huguenard, J.R.,
815 Hegemann, P., Deisseroth, K., 2011. Neocortical excitation/inhibition balance in
816 information processing and social dysfunction. Nature 477, 171-178.
817 Young, K.S., Parsons, C.E., Stein, A., Kringelbach, M.L., 2015. Motion and emotion: depression
818 reduces psychomotor performance and alters affective movements in caregiving

819 interactions. Frontiers in behavioral neuroscience 9, 26.

820 Yu, P., An, S., Tai, F., Zhang, X., He, F., Wang, J., An, X., Wu, R., 2012. The effects of neonatal

821 paternal deprivation on pair bonding, NAcc dopamine receptor mRNA expression and

822 serum corticosterone in mandarin voles. Hormones and behavior 61, 669-677.

823 Yuan, Y., Wu, W., Chen, M., Cai, F., Fan, C., Shen, W., Sun, W., Hu, J., 2019. Reward Inhibits

824 Paraventricular CRH Neurons to Relieve Stress. Current biology : CB 29, 1243-1251

825 e1244.

826 Zhao, S., Ting, J.T., Atallah, H.E., Qiu, L., Tan, J., Gloss, B., Augustine, G.J., Deisseroth, K., Luo,

827 M., Graybiel, A.M., Feng, G., 2011. Cell type-specific channelrhodopsin-2 transgenic mice

828 for optogenetic dissection of neural circuitry function. Nature methods 8, 745-752.

829

830

831

832 **SUPPLEMENTARY 1. SUPPLEMENTAL FIGURES.**

833

834 **Figure 1—figure supplement 1. The histology of CTB injecting into the right ACC of male (up**

835 **row) and female voles (down row).** The right panels showed colocalization of TPH2^{+} neurons

836 (green) and CTB (red) in the DR (× 200). M: male; F: female; ACC: anterior cingulate cortex; DR:

837 dorsal raphe nucleus; TPH2: tryptophan hydroxylase 2; Aq: aqueduct.

838

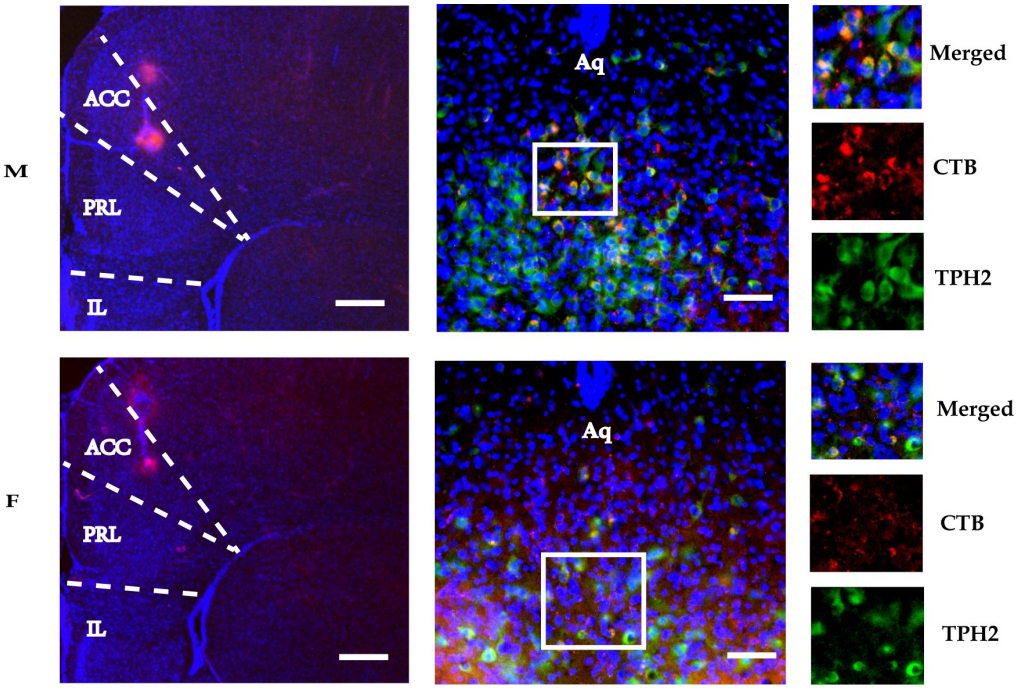

839

840

841 **Figure 1—figure supplement 2. Immunohistological images showing colocalization of opsins**
842 **(mCherry, red), TPH2+ neurons (green) and DAPI (blue) in the DR of males (A) and (B)**
843 **females voles.** (a1 & b1): merged image of DAPI and mCherry (× 100); (a2-a4, b2-b4): amplified
844 images in the left box showing the mCherry, TPH2 and the colocaliztion of mCherry and TPH2
845 (× 200); (a5, b5): quantification rates of mCherry neurons colabled with TPH2 (left pies), and
846 TPH2 neurons colabled with mCherry (right pies), n = 3 in each sex. DR: dorsal raphe nucleus;
847 TPH2: tryptophan hydroxylase 2.
848

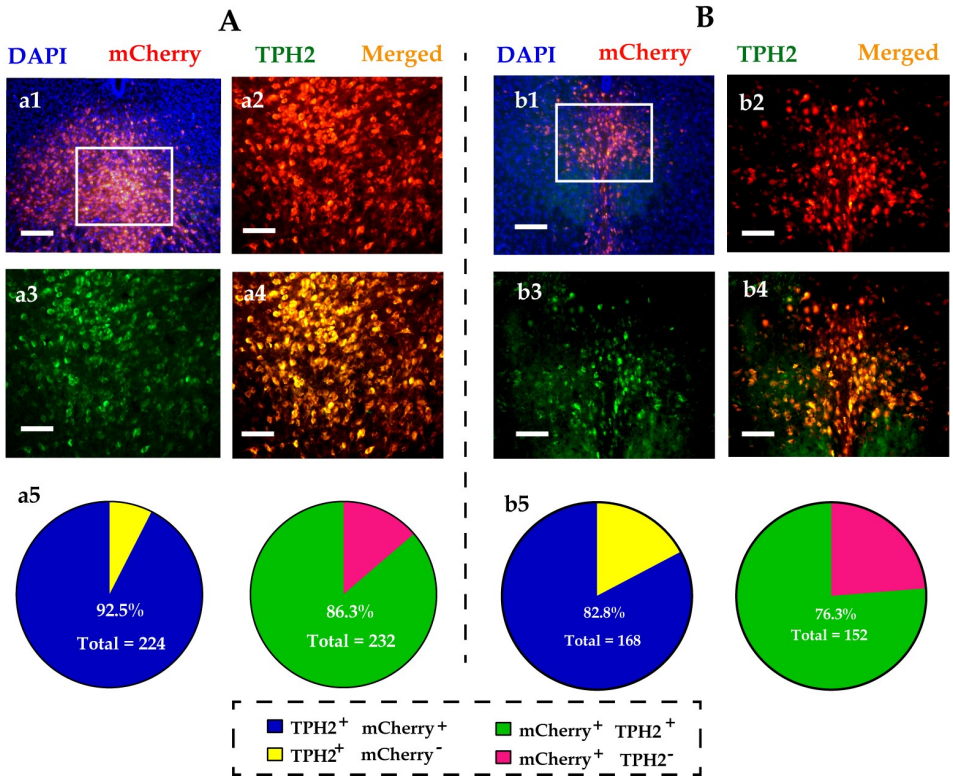

849
850
851
852
853
854

Figure 1—figure supplement 3. Schematics depict virus spread (shades) and optic fiber placements (lines) for recording and functional manipulation experiments, related to figures 1, 3, 4 and 5 (A, B C and D, respectively).

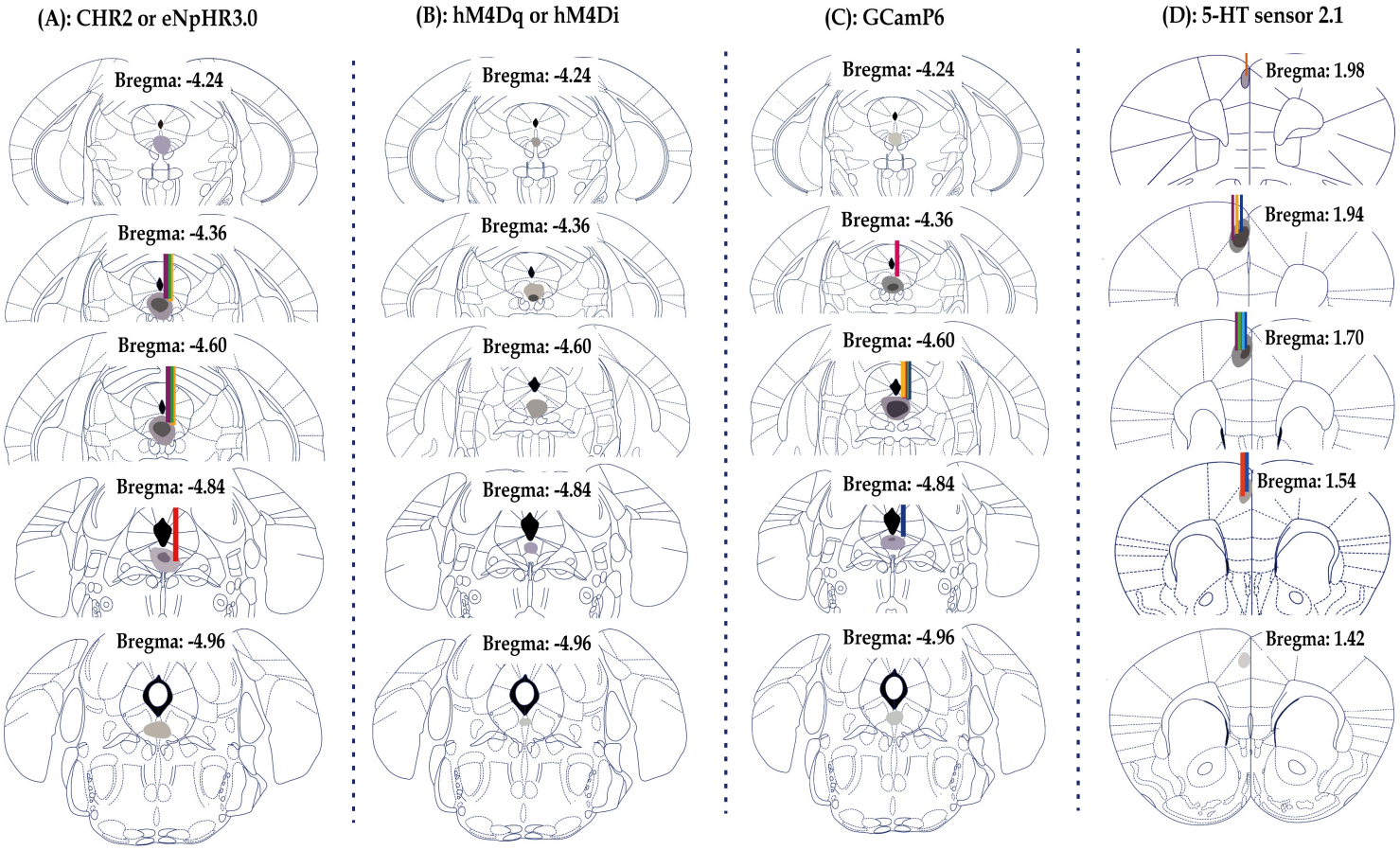

1 **Figure 1—figure supplement 4. Effect of bidirectional optogenetic modulation of DR 5-HT**

2 **neuron activities in the DR-ACC neural circuit on some control behaviors.** Quantification of

3 chasing time (A & B) and grooming time (C & D) in the consolation test; and the distance

4 traveled in the open-field test (E & F). Data are presented as mean ± SE, n = 7–8 in each group,

5 $^{**}P < 0.01$. For A-D, Independent samples t test and Bayesian samples t-test; for E-F, two-way

6 repeated ANOVA and two-way Bayesian Repeated Measures ANOVA (light as within subject

7 factors). ACC: anterior cingulate cortex; CTR: control; DR: dorsal raphe nucleus.

8

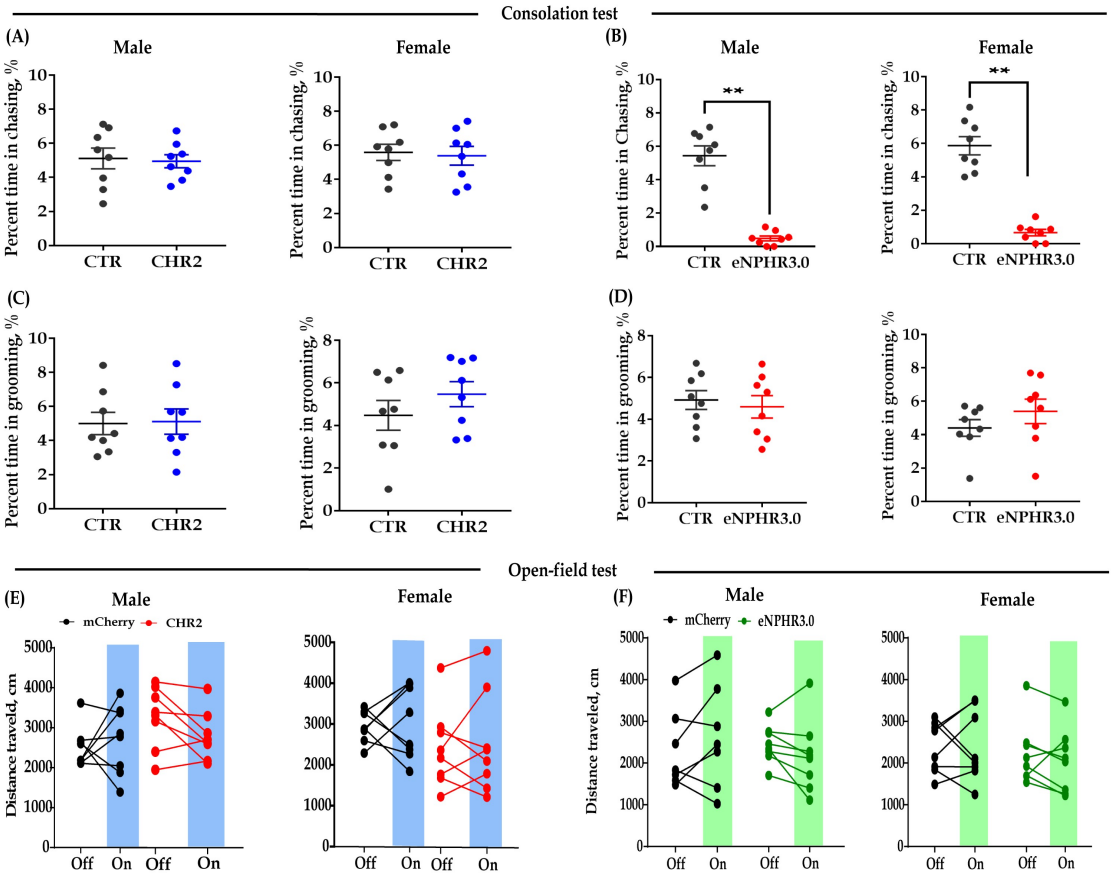

9

10

11 **Figure 1—figure supplement 5. Effect of optogenetic inhibition of DR 5-HT neurons in the**

12 **DR-ACC neural circuit does not elicit long-lasting effects (< 24 h) on allogrooming and**

13 **chasing behavior in the consolation test.** The data are derived from Figure 1H. (A): Time

14 spent in allogrooming; (B) allogrooming frequency; (C): time spent in chasing and chasing

15 frequency (D). Data are presented as mean ± SE, n = 8 in each group; Paired sample t-test and

16 Bayesian Paired samples t-test; $^{**}P < 0.01$. ACC: anterior cingulate cortex; DR: dorsal raphe

17 nucleus; CTR: control.

18

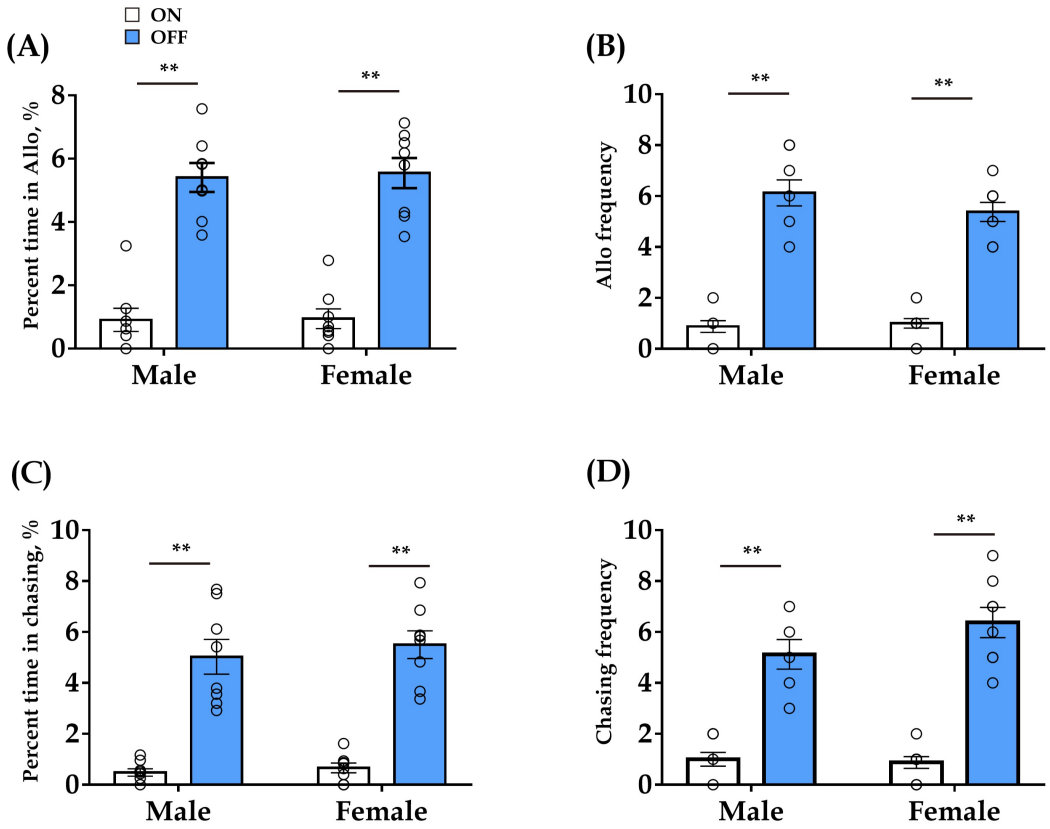

19

20

21 **Figure 2—figure supplement 1. Effect of bidirectional optogenetic modulation of ACC 5-HT**

22 **terminals in the DR-ACC neural circuit on some control behaviors.** Quantification of chasing

23 time (A & B) and grooming time (C & D) in the consolation test and the distance traveled in the

24 open-field test (E & F). Data are presented as mean ± SE, n = 7–8 in each group, **P < 0.01. For

25 A-D, Independent samples t test and Bayesian samples t-test; for E-F, two-way repeated

26 ANOVA and two-way Bayesian Repeated Measures ANOVA (light as within subject factors).

27 ACC: anterior cingulate cortex; DR: dorsal raphe nucleus; CTR: control.

28

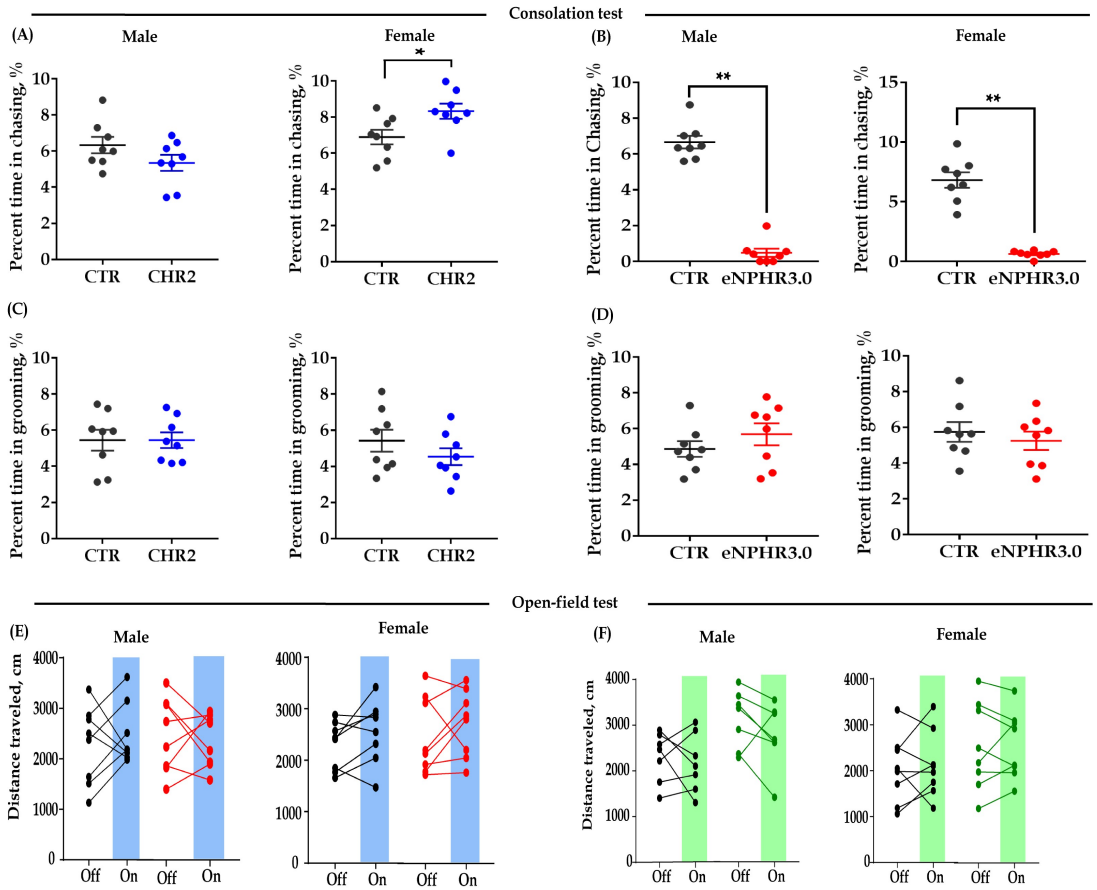

29

30 **Figure 2—figure supplement 2. Effect of optogenetic inhibition of ACC 5-HT terminals in**

31 **the DR-ACC neural circuit does not elicit long-lasting effects (< 24 h) on allogrooming and**

32 **chasing behaviors in the consolation test.** The data are derived from Figure 2D. (A): Time

33 spent in allogrooming; (B) allogrooming frequency; (C): time spent in chasing; (D): chasing

34 frequency. Data are presented as mean ± SE, n = 7–8 in each group; Paired sample t-test and

35 Bayesian Paired samples t-test; $^{**}P < 0.01$. ACC: anterior cingulate cortex; DR: dorsal raphe

36 nucleus; CTR: control; Allo: allogrooming.

37

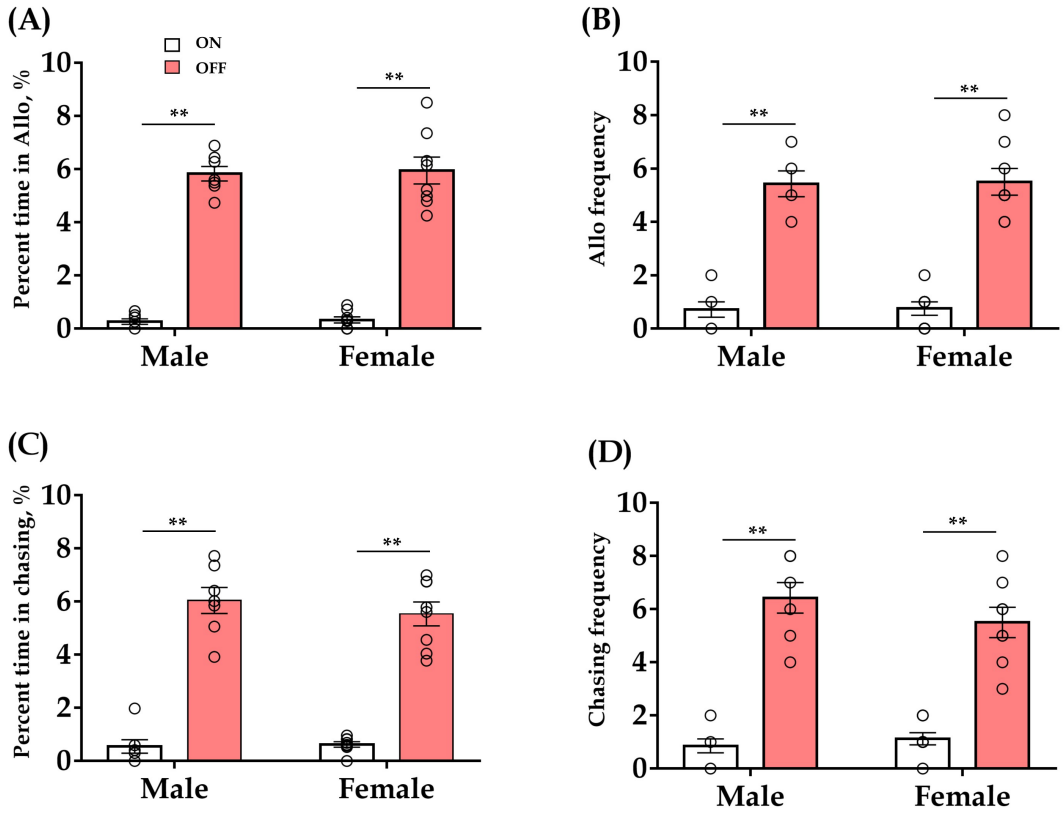

38

39

40

41 **Figure 3—figure supplement 1. Immunohistological image showing colocalization of**

42 **DREADD (mCherry, red), TPH2+ neurons (green) and DAPI (blue) in the DR of male (A)**

43 **and (B) female voles.** (a1 & b1): merged image of DAPI and mCherry (× 100); (a2-a4, b2-b4):

44 amplified images in the left box showing the mCherry, TPH2 and the colocaliztion of mCherry

45 and TPH2 (× 200); (a5, b5): quantification rates of mCherry neurons colabled with TPH2 (left

46 pies), and TPH2 neurons colabled with mCherry (right pies), n = 3 in each sex. TPH2:

47 tryptophan hydroxylase 2.

48

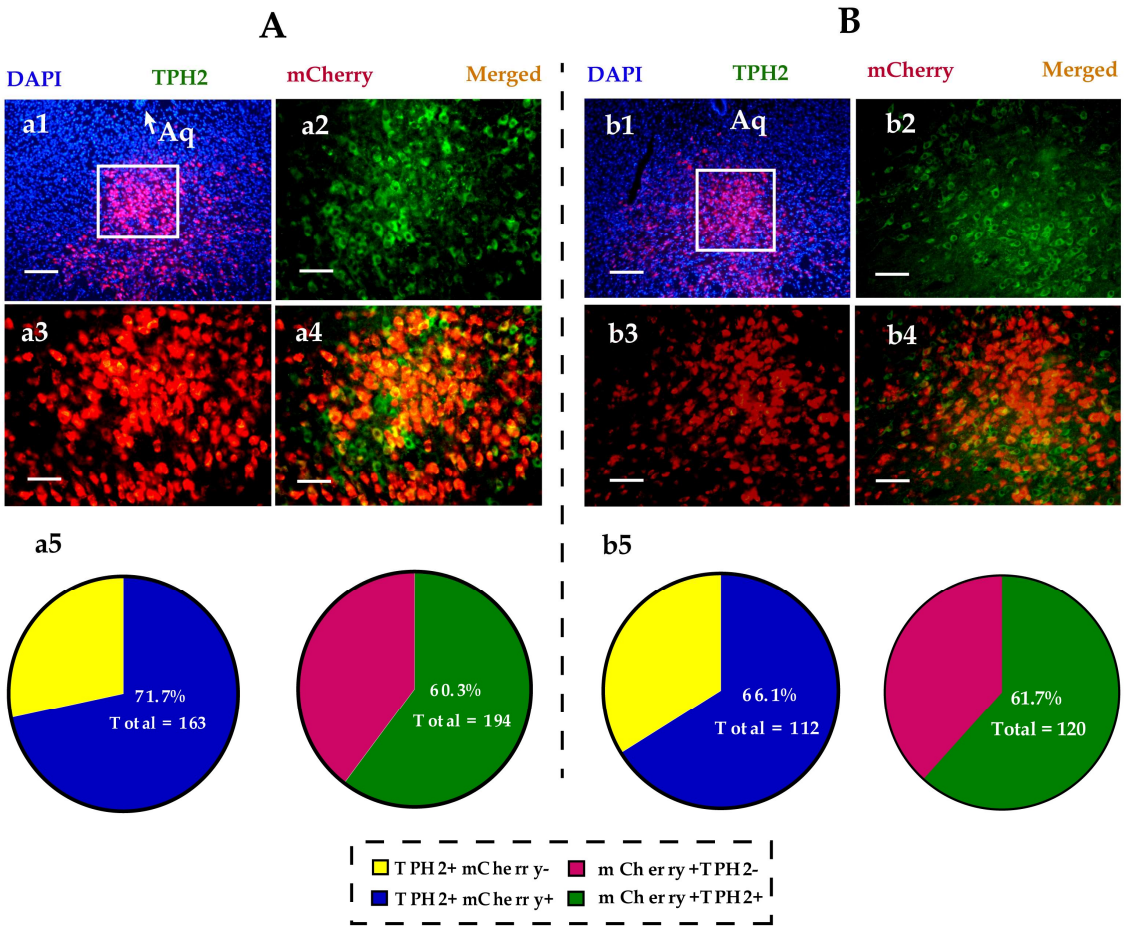

49

50

51 **Figure 3—figure supplement 2. Effect of chemogenetic modulation of DR 5-HT neuron**

52 **activities in the DR-ACC neural circuit on some control behaviors.** Quantification of chasing

53 time (A) and grooming time (B) in the consolation test, and distance traveled in the open-field

54 test (C). Data are presented as mean ± SE, *n* = 7–8 in each group; two-way repeated measures

55 ANOVA along with two-way Bayesian repeated measures ANOVA. ACC: anterior cingulate

56 cortex; DR: dorsal raphe nucleus; M: male; F: female; OFT: open-field test.

57

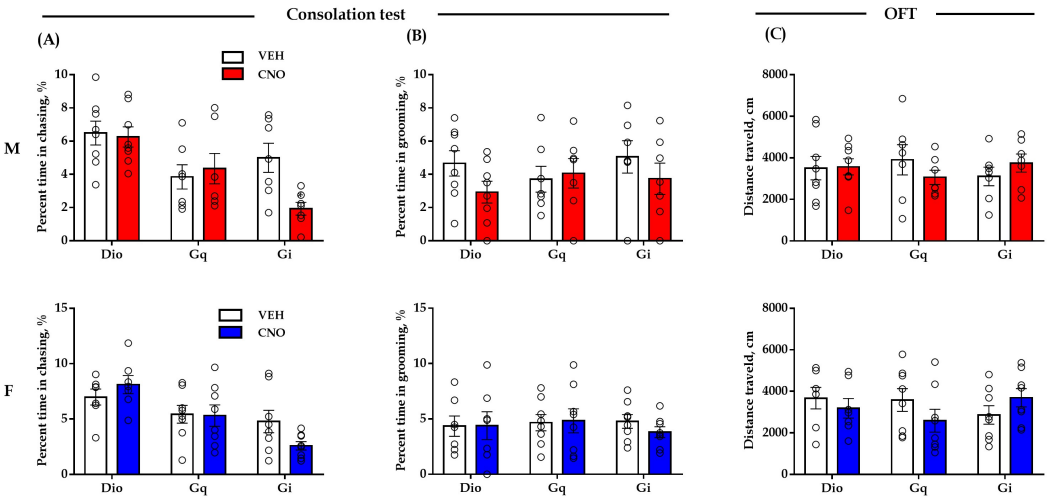

58

59

Figure 4—figure supplement 1. Representative viral infection images of GCaMp6. (a1): Immunohistological image showing GCaMP6 expression in the DR (× 100); (a2-a4): amplified images in the left box showing the GCaMP6 (green), TPH2 (red) and the colocaliztion (yellow) of the two (× 200); (a5): quantification rates of GCaMP6 neurons colabled with TPH2 (left pie), and TPH2 neurons colabled with GCaMP6 (right pie), n = 3; (b1): immunohistological image showing GFP expression in the DR (× 100); (b2-b4): amplified images in the left box showing the GFP (green), TPH2 (red) and the colocaliztion (yellow) of the two (× 200); (b5): quantification rates of GFP neurons colabled with TPH2 (left pie), and TPH2 neurons colabled with GFP (right pie), n = 3.

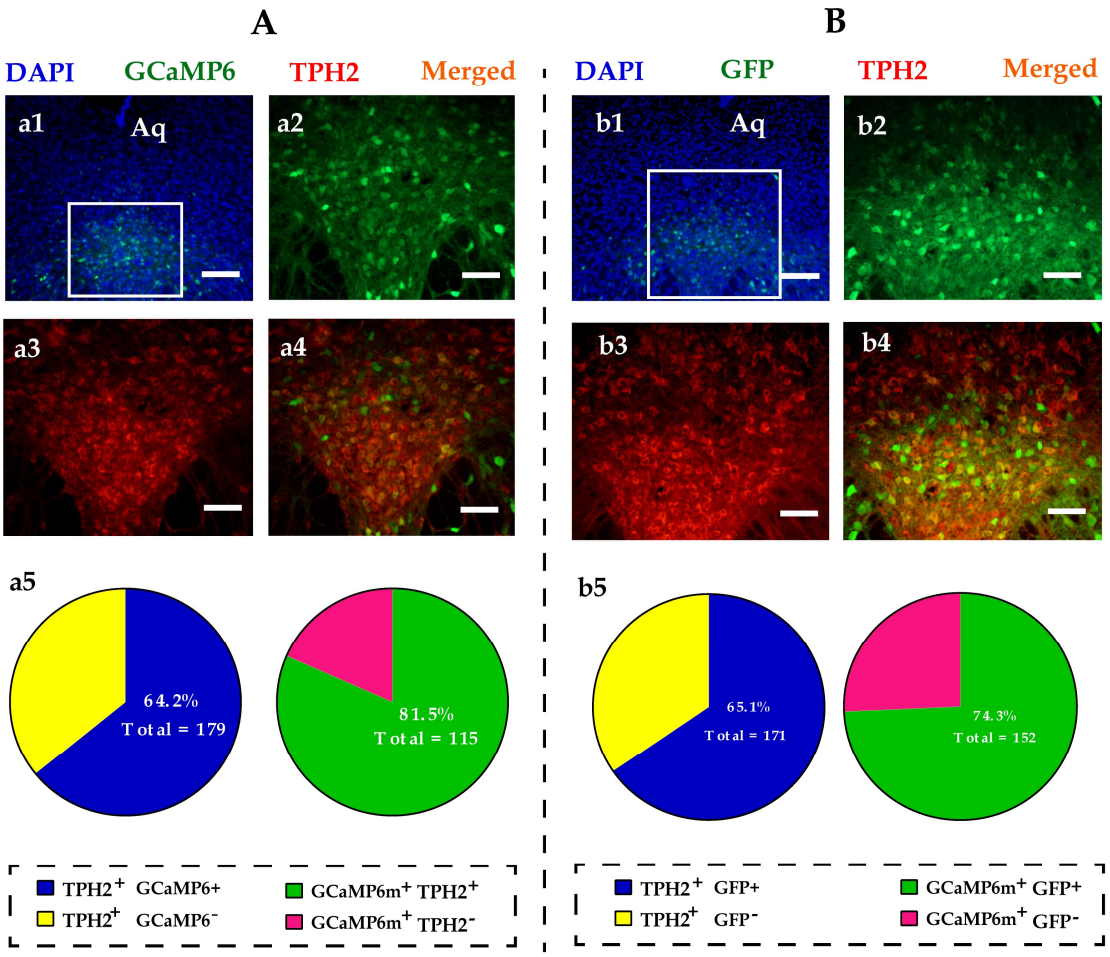

Figure 4—figure supplement 2. Peak GCaMP6 (A & B) and 5-HT sensor (C & D) fluorescence values during a few of behaviors in both male and female voles. Data are presented as mean ± SE, *n* = 6 in each group. Groups not sharing the same letter significantly differ from each other; one-way ANOVA along with one-way Bayesian ANOVA. Allo: allogrooming; Sni: sniffing; App: social approaching; Gro: selfgrooming; Run: running.

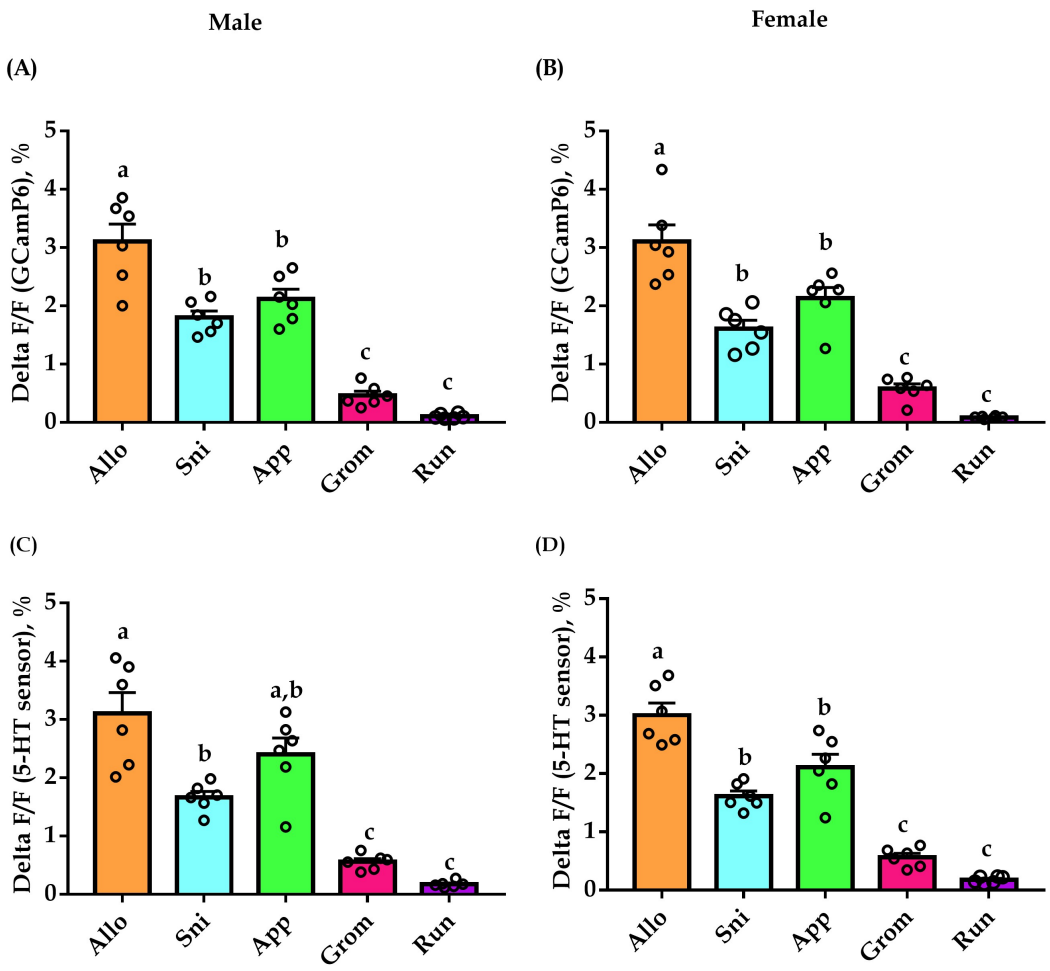

Figure 4—figure supplement 3. GCaMP6 fluorescent signals align to the end of some behaviors. (A1, B1, C1): Representative peri-event plot of GCaMP6 fluorescence signals aligned to the end of allogrooming, social approaching and sniffing (for all peri-event plots, the red line denotes the mean signals of 4-6 bouts of behaviors, whereas the red shaded region denotes the SE); (A2, B2, C2): quantification of change in GCaMP6 fluorescence signals. Data are presented as mean ± SE, *$P < 0.05$, **$P < 0.01$, $n = 6$ in each group; paired samples t test along with Bayesian paired samples t-Test. ALLO: allogrooming; APP: approaching; SNI: sniffing.

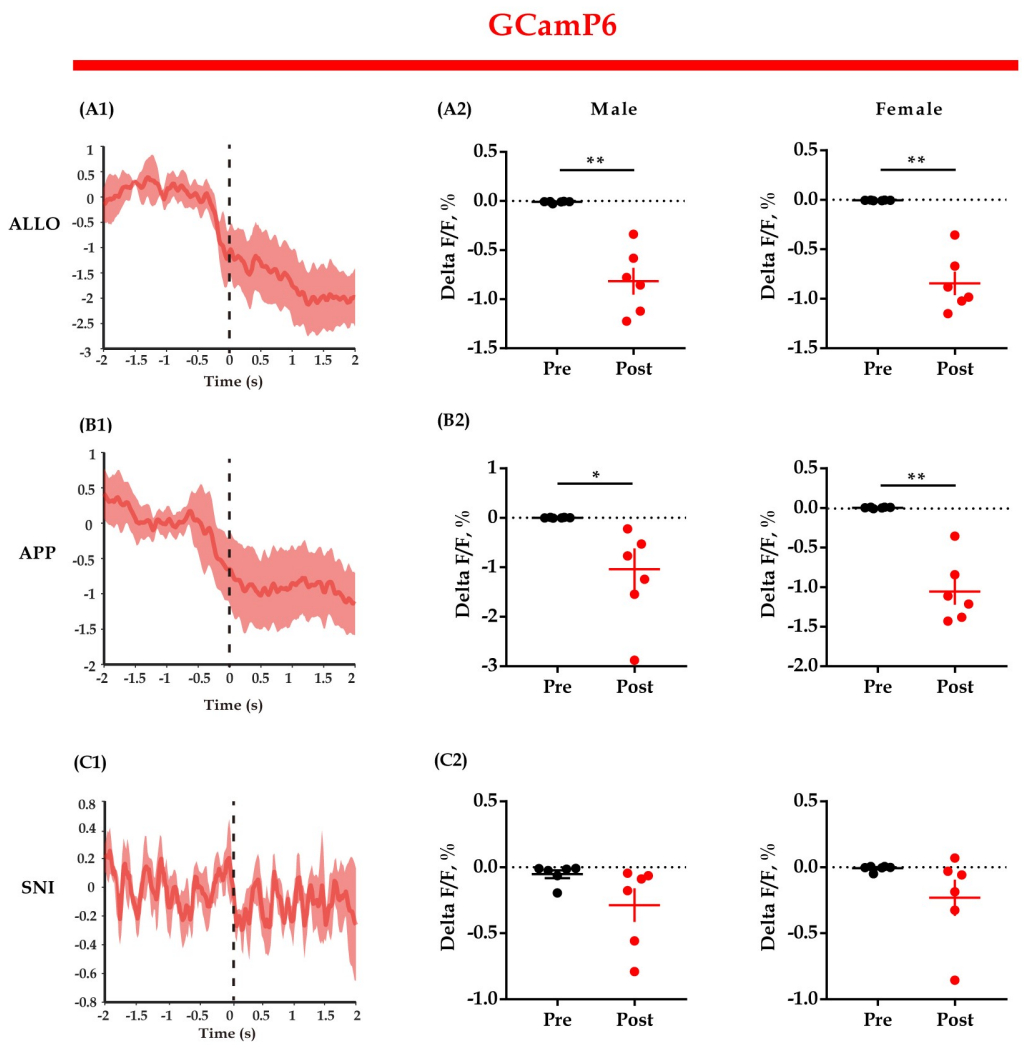

Figure 5—figure supplement 1. 5-HT sensor fluorescent signals align to the end of some behaviors. (A1, B1, C1): Representative peri-event plot of 5-HT sensor fluorescence signals aligned to the end of allogrooming, social approaching and sniffing (for all peri-event plots, the blue line denotes the mean signals of 4-6 bouts of behaviors, whereas the blue shaded region denotes the SE); (A2, B2, C2): quantification of change in 5-HT sensor fluorescence signals. Data are presented as mean ± SE, $*P < 0.05$, $**P < 0.01$, $n = 6$ in each group; simple Paired t test along with Bayesian Paired Samples t-Test. ALLO: allogrooming; APP: approaching; SNI: sniffing.

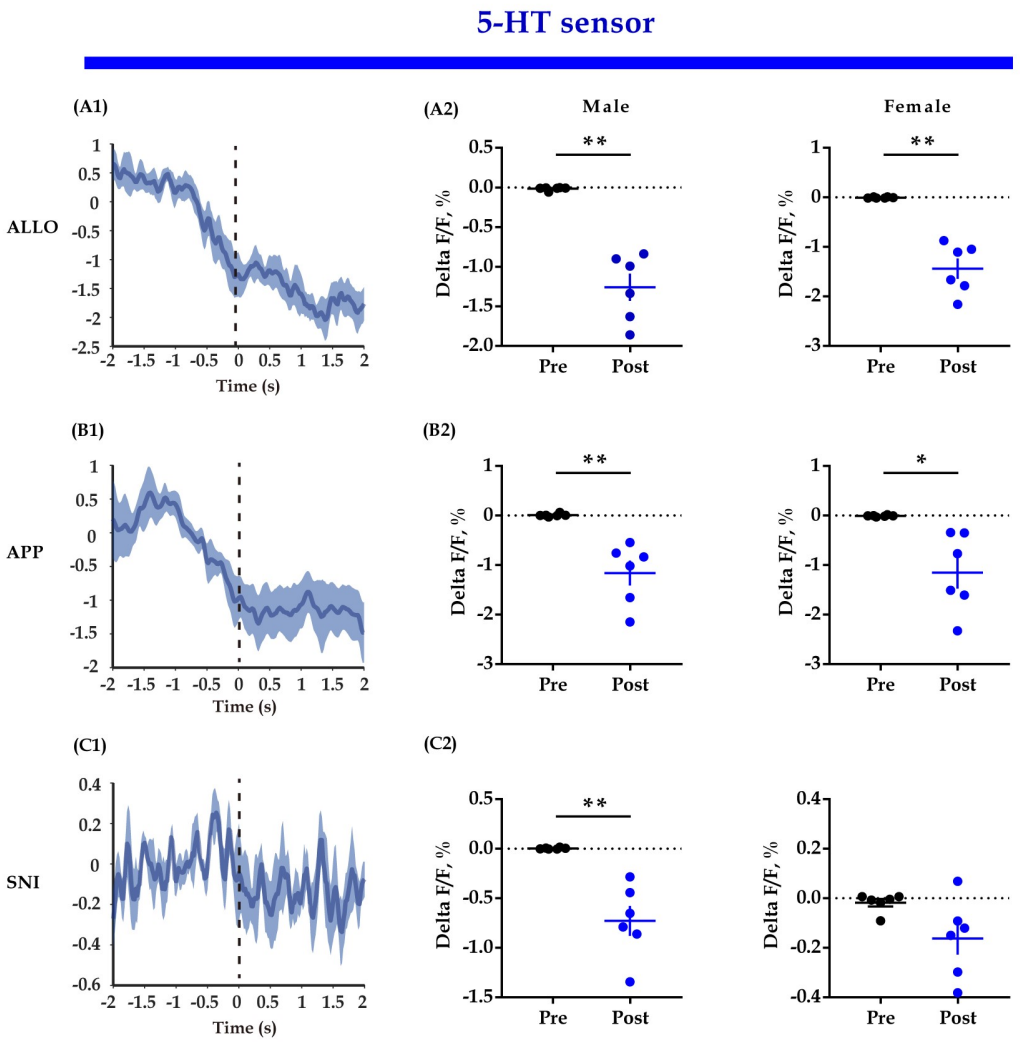

Figure 5—figure supplement 2. 5-HT sensor fluoresce changes during allogrooming could be blocked by Met. (A): Schematic diagrams; (B): combined individual 5-HT sensor fluorescence traces during allogrooming in response to Met (blue) or Veh (red); (C, D): quantification of 5-HT sensor fluorescence signals during allogrooming in response to Met or Veh in male (C) and female subjects. Data are presented as mean ± SE, $^{**}P < 0.01$, $n = 6$ in each group; two-way Repeated measures ANOVA and two-way Bayesian repeated measures ANOVA. Met: metergoline, a 5-HT receptor antagonist; Veh: vehicle.

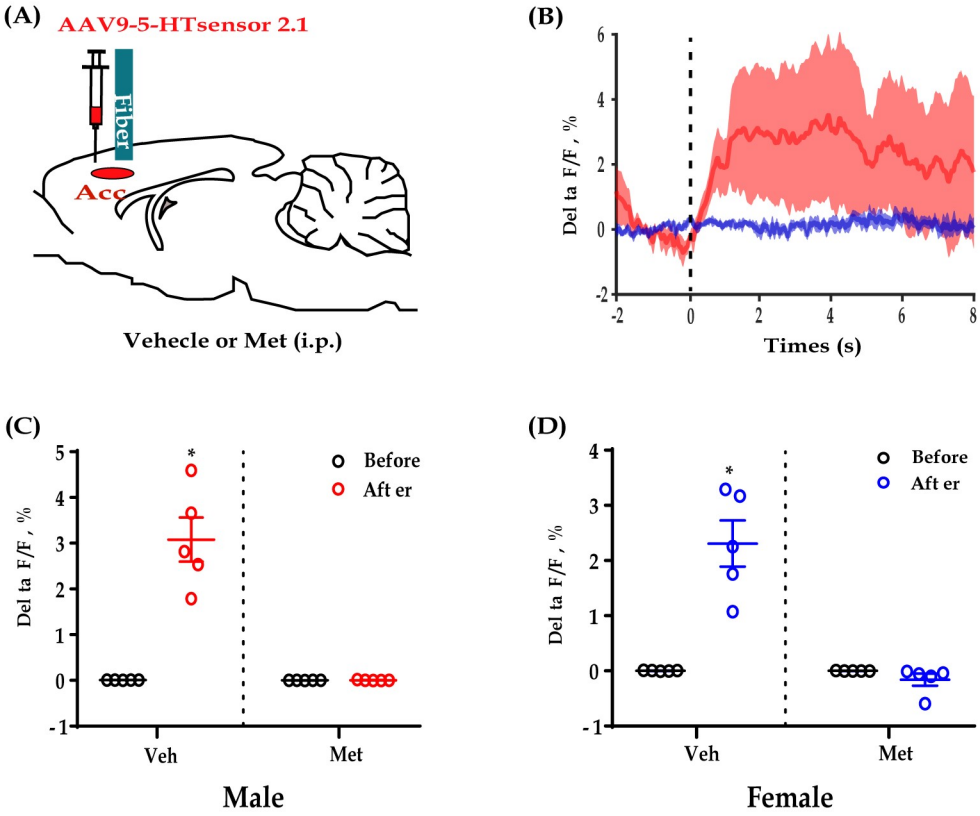

121 **Figure 6—figure supplement 1. Comparisons of 'Vehicle+Saline - Vehicle+CNO' vs**

122 **'8-OH-DPAT+Saline - 8-OH-DPAT+CNO' (A & B) and 'Vehicle+Saline - Vehicle+CNO' vs**

123 **'MDL 100907+Saline - MDL 100907+CNO' (C & D).** Independent samples *t*-test and Bayesian

124 independent samples *t*-test. N = 5-6 in each group, *P < 0.05.

125

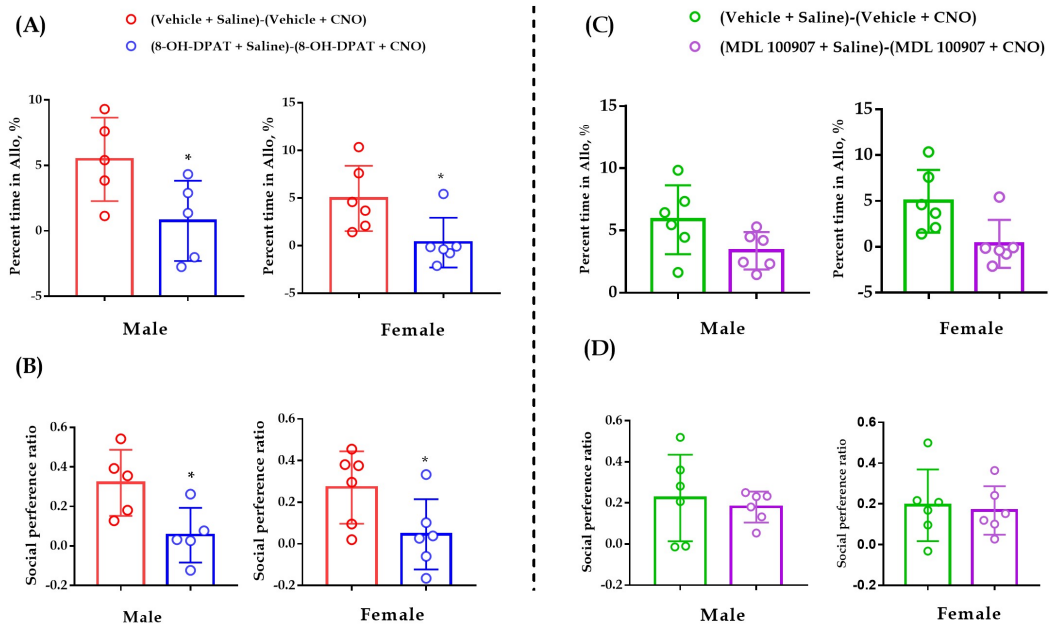

126

127

128 **Figure 6—figure supplement 2. Chemogenetic inhibition of DR 5-HT neuron in the**

129 **DR-ACC neural circuit along with intra-ACC injection of 5-HT1AR agonist (8-OH-DPAT) or**

130 **5-HT2AR antagonist (MDL 100907) had no significant effect on control behaviors of**

131 **selfgrooming (A, C) and distance traveled in the open-field test (B, D).** Two-way ANOVA

132 and two-way Bayesian ANOVA. *N* = 5-6 in each group. ACC: anterior cingulate cortex; DR:

133 dorsal raphe nucleus; M: male; F: female.

134

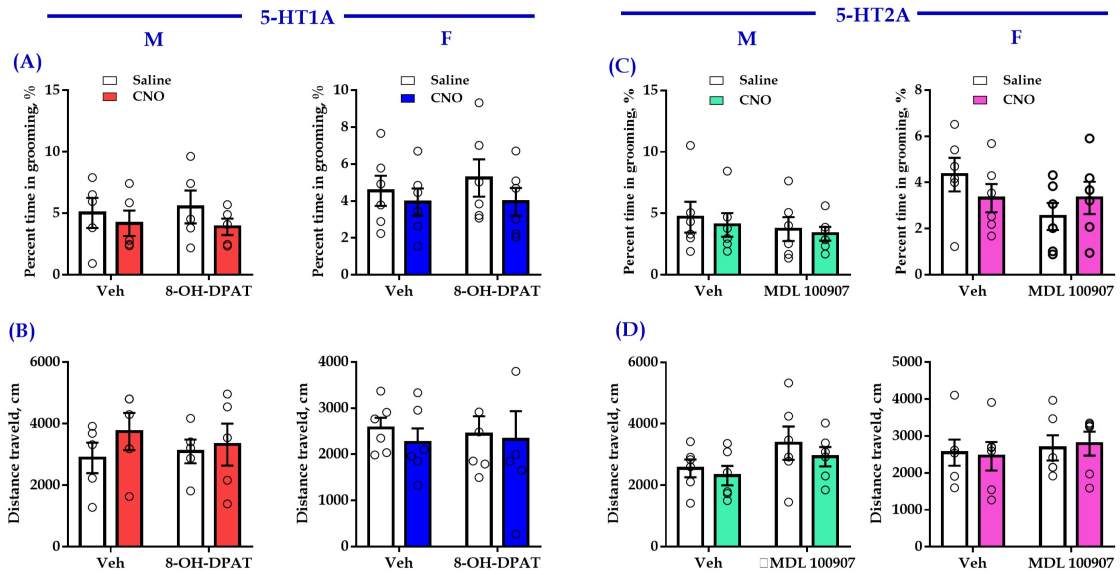

135

136

137